Discotic liquid crystals: a new generation of organic semiconductors†

Sergey Sergeyev,[a] Wojciech Pisula[b] and Yves Henri Geerts*[a]

Received 23rd April 2007
First published as an Advance Article on the web 3rd July 2007
DOI: 10.1039/b417320c

Discotic (disc-like) molecules typically comprising a rigid aromatic core and flexible peripheral chains have been attracting growing interest because of their fundamental importance as model systems for the study of charge and energy transport and due to the possibilities of their application in organic electronic devices. This *critical review* covers various aspects of recent research on discotic liquid crystals, in particular, molecular design concepts, supramolecular structure, processing into ordered thin films and fabrication of electronic devices. The chemical structure of the conjugated core of discotic molecules governs, to a large extent, their intramolecular electronic properties. Variation of the peripheral flexible chains and of the aromatic core is decisive for the tuning of self-assembly in solution and in bulk. Supramolecular organization of discotic molecules can be effectively controlled by the choice of the processing methods. In particular, approaches to obtain suitable macroscopic orientations of columnar superstructures on surfaces, that is, planar uniaxial or homeotropic alignment, are discussed together with appropriate processing techniques. Finally, an overview of charge transport in discotic materials and their application in optoelectronic devices is given (234 references).

1. Introduction

Organic electronics, *i.e.* the use of conjugated molecules as active components in electronic devices, is a field of intense scientific activity because of the prospect of the creation of a new industry. Electronic devices such as light-emitting-diodes (LED), photovoltaic diodes (PVD), field effect transistors (FET), memory elements and sensors are now commonly encountered in the chemical literature. The reason for this is twofold. On the one hand, the interest in devices is driven by the potential applications. On the other hand, devices are formidable tools to probe the basic structure–performance relationships that govern the physics and chemistry of organic semiconductors. This challenge also creates a need for new conjugated materials with innovative design and semiconducting behavior that deviates from that of rather conventional conjugated materials, *i.e.* linear oligomers and polymers.[1,2] Hierarchical self-assembly of molecules into supramolecular systems leads to alternative classes of functional materials.[3–5]

[a]*Université Libre de Bruxelles, Laboratoire de Chimie des Polymères, CP206/1, Boulevard du Triomphe, 1050, Brussels, Belgium. E-mail: ygeerts@ulb.ac.be.*
[b]*Max Planck Institute for Polymer Research, Ackermannweg 10, 55128, Mainz, Germany*
† Dedicated to Prof. Klaus Müllen on the occasion of his 60th birthday.

Sergey Sergeyev

Sergey Sergeyev received his MSc in chemistry from Lomonosov Moscow State University, Russia and his PhD in chemistry from the University of Zürich, Switzerland. During his postdoctoral training with François Diederich at ETH Zürich he worked on stereoselective functionalization of fullerenes. In 2004 he joined the group of Yves Geerts at the Université Libre de Bruxelles (ULB), Belgium, as a research associate. In addition to discotic and calamitic mesogens, his current research interests include chromophores for NLO applications, the synthetic chemistry of Tröger's base and other cleft-like molecules as well as their applications towards asymmetric catalysis and molecular recognition.

Wojciech Pisula

Wojciech Pisula studied chemical engineering at Osnabrück University of Applied Sciences, Germany and at the University of Wales, Swansea, where he received his MSc degree. In 2001, he joined the group of Klaus Müllen at the Max Planck Institute for Polymer Research (MPIP) in Mainz, Germany, where he completed his PhD thesis in 2005. His research was focused on the control of the supramolecular self-organization of discotic liquid crystalline polycyclic aromatic hydrocarbons with a strong interest on their application in electronic devices. After an additional year as a postdoctoral scientist in the same group, he has been employed in the process technology and engineering department of Degussa, Germany. He keeps the status of guest scientist at the MPIP.

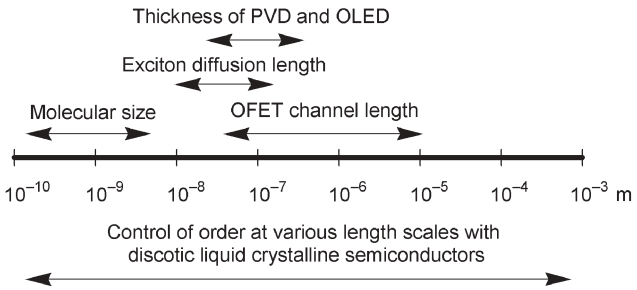

Fig. 1 Typical length scales encountered in organic electronics and control of order achievable with LC semiconductors.

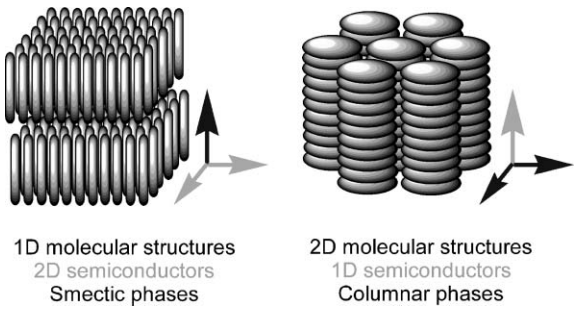

Fig. 2 Schematic drawing of calamitic (left) and discotic (right) semiconductors.

Amongst the various new materials for organic electronics, conjugated liquid crystals (LCs) are currently viewed as a new generation of organic semiconductors because they bring *order* and *dynamics*.[6] Order is likely the most important parameter that governs the performances of organic semiconductors in devices. Conjugated LCs offer the decisive advantage of controlling order in the bulk and at interfaces, and at all length scales from molecular to macroscopic distances (see Fig. 1). The role of dynamics in organic semiconductors is also important but less explored. The most striking example of the effect of dynamics is the ability of conjugated liquid crystals to self-heal structural defects such as grain boundaries due to their liquid-like character. Upon simple thermal annealing, it is common to observe the spontaneous formation of *large single domains* that extend over several square mm, for films up to several μm thick.[7,8] The orientation of molecules within these large domains can be manipulated by various means, such as a concentration or temperature gradient,[9,10] irradiation with polarized light,[11] or surface alignment layers.[12–14]

The ease of alignment into single domains arises from the fact that conjugated LCs are composed of small organic molecules that form phases of low inherent viscosity. The low molecular weight of conjugated LCs associated with discrete mass allows the synthesis of defect-free chemical structures that are amenable to a higher purity level than most conjugated polymers.[1]

Amongst the conjugated LCs one should differentiate the calamitic (rod-like)[15,16] from the discotic (disc-like) mesogens.[5] They differ in their molecular shape, their phase symmetry, the dimensionality of their charge transport and exciton migration and in the extent of their orbital overlap (Fig. 2). Calamitics tend to form smectic mesophases whereas discotics self-organize into columnar mesophases. Smectic planes demonstrate a two-dimensional charge transport comparable to that observed for the herringbone packing of pentacene and oligothiophenes.[17] As a result, the extent of frontier orbital overlap is rather moderate. Typically, the band width of calamitics is expected to be below the corresponding value for pentacene, a well-studied low molecular weight organic crystalline semiconductor (*ca.* 0.5–0.6 eV).[18]

The two-dimensional chemical structure of discotics creates a new situation that results in a set of unusual features. Columns of discotic mesogens exhibit one-dimensional charge transport that is rather sensitive to the structural defects. These defects such as "Y" bifurcation can be visualized with high resolution microscopy techniques as the disc diameter is *ca.* 2–3 nm.[9] Discotic semiconductors thus appear to be a unique system which enables correlation of the occurrence of defects with charge transport properties. Moreover, within the columns adjacent disc-like molecules experience a much larger orbital overlap than calamitics. The band width reaches values as high as 1.1 eV, *i.e.* close to that of graphite (*ca.* 1.0–1.4 eV).[19] The large orbital overlap between stacked disc-like molecules is reflected in the high values of the *charge carrier mobility* (μ), *i.e.* 0.2–1.3 $cm^2\ V^{-1}\ s^{-1}$, in their liquid crystalline (LC) mesophases.[20–23] In the same columnar mesophases, the *exciton diffusion length* (l_e) in discotics exceeds 70 nm.[24] This is one order of magnitude higher than for most of conventional conjugated polymers. The two-dimensional structure associated with the disc shape allows one to tailor the emissive properties by the control of the mutual orientation of transition dipoles upon rotation of the discs.[17] This paves the way to columnar mesophases that combine high charge carrier mobility with intense fluorescence.[25,26]

The unique features of discotic semiconductors briefly mentioned in this introduction will be documented in the next sections and in the light of underlying molecular concepts, supramolecular order, processing into thin films, and device

Yves Henri Geerts

Yves Henri Geerts was born in Brussels in 1967. He accomplished his diploma studies with Jean-Pierre Sauvage at the Université Louis Pasteur in Strasbourg, France. In 1993, he obtained his PhD degree from Université Libre de Bruxelles (ULB), Belgium. After postdoctoral studies with Klaus Müllen at the Max Planck Institute for Polymer Research (MPIP) in Mainz, Germany and with Richard Schrock at MIT in Boston, USA he spent two more years at MPIP as a research associate. In 1997, he returned to Belgium and accepted the tenured position of Belgian Scientific Research Foundation (FNRS) Fellow at ULB. In 1999 he was appointed Professor at the same university. His current research focuses on synthesis, self-assembly and processing of calamitic and discotic liquid crystals and is directed towards their application in electronic devices.

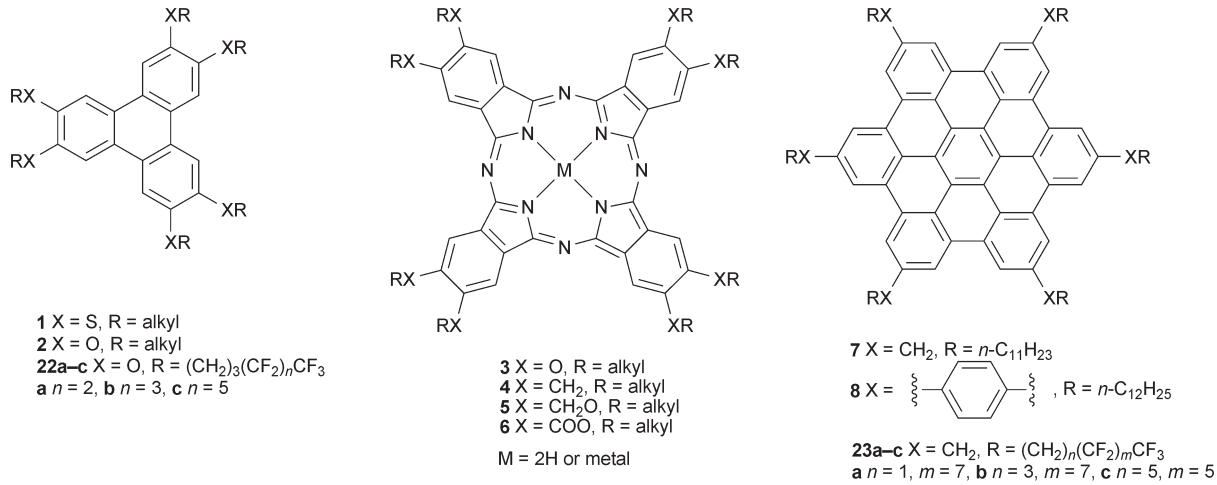

Fig. 3 Selected examples of widely studied discotic molecules; R = alkyl.

performance. The focus will be largely on unprecedented molecular structures that have not been a topic of the earlier extensive reviews.[27–37]

2. Molecular concepts

Although some early work on discotic LCs as semiconductors was conducted in the 1980s,[38] the decisive discovery dates back to 1994 and to the work of Adam *et al.*[39] They showed, using time-of-flight photoconductivity (TOF) experiments, that hexahexylthiotriphenylene **1** (Fig. 3) has a charge carrier mobility of holes (μ_+) of *ca.* 0.1 $cm^2\ V^{-1}\ s^{-1}$ in a particularly rare helical mesophase.[39] These results were soon after confirmed by van de Craats *et al.* with the electrode-less pulse-radiolysis time resolved microwave conductivity (PR-TRMC) method.[40,41]

Theoreticians have rationalized the various experimental observations of charge transport into a coherent view based on the Marcus equation.[42] According to this theoretical description, the electron hopping rate between adjacent discs is explained in terms of two molecular parameters: (i) the transfer integral which is a function of the overlap of HOMO (LUMO) orbitals of adjacent molecules for hole (electron) transport, and (ii) the internal reorganization energy (λ_i) associated with the energy difference between charged and neutral species.[42] Beside efficient charge transport, the interest in discotic LCs has originated from the ability of discotics to carry excitons over large distances. Detailed spectroscopic studies have been pursued by Markovitsi *et al.* to determine the values of l_e as a function of chemical structure, phase, and temperature.[24]

In parallel with physical and theoretical investigations, the field of discotic LCs has mainly been synthetically driven to bring the structural diversity needed to establish reliable structure–property relationships. Several molecular concepts have been explored: (i) the chemical structure, symmetry and size of the conjugated core, (ii) the shape of the wavefunctions, (iii) the nature of the connecting groups between the conjugated core and the flexible side chains, and (iv) the phase and transition temperature engineering by the variation of peripheral substituents. In the next sections, these molecular concepts are analyzed and discussed in the light of the most recent publications.

2.1 Size of the conjugated core

Early studies of discotic molecules began with the smallest possible aromatic core, *i.e.* benzene.[29] It soon became evident that larger cores prone to more efficient π-stacking are necessary, and not surprisingly, variation of the *size* of the conjugated core is one of the major aspects explored so far in the design of discotic mesogens. Various larger disc-like molecules, such as the triphenylene derivatives **1** and **2** mentioned above have been extensively studied.[29] The importance of phthalocyanines (Pc) in the field of dyes and pigments due to their extraordinary thermal and photochemical stability prompted the synthesis of LC phthalocyanine derivatives such as **3–6**.[43–47] Several examples of porphyrin discotics and their use in electronic devices are known. They have been a topic of previous reviews.[32,48]

The synthesis of hexaalkyl hexa-*peri*-hexabenzocoronene (HBC) derivatives **7** and **8** in the mid-nineties[49] can be considered as an important achievement not only because of the record charge carrier mobility values but also since it has paved the way to very large liquid crystalline polycyclic aromatic hydrocarbons (PAHs) shown in Fig. 4.[50] The unprecedented PAHs **9–13** contain from 24 to 132 aromatic carbon atoms[5,51–53] (see also Table 1) and can be viewed as graphite subunits. They offer an excellent opportunity to discuss the diameter of the conjugated core as a key parameter for charge transport.[54] On the basis of the charge mobility value for different discotics, van de Craats and Warman suggested the following empirical relationship:

$$\Sigma\mu_{1D} = 3\exp(-83/n)\ cm^2\ V^{-1}\ s^{-1}$$

where $\Sigma\mu_{1D}$ is a mobility sum for holes (μ_+) and electrons (μ_-) along the axis of the columnar stacks and n is the number of carbon atoms in the aromatic core. The value of 3 $cm^2\ V^{-1}\ s^{-1}$ is the charge carrier mobility found for the interlayer charge transport in graphite which is considered as the maximum mobility

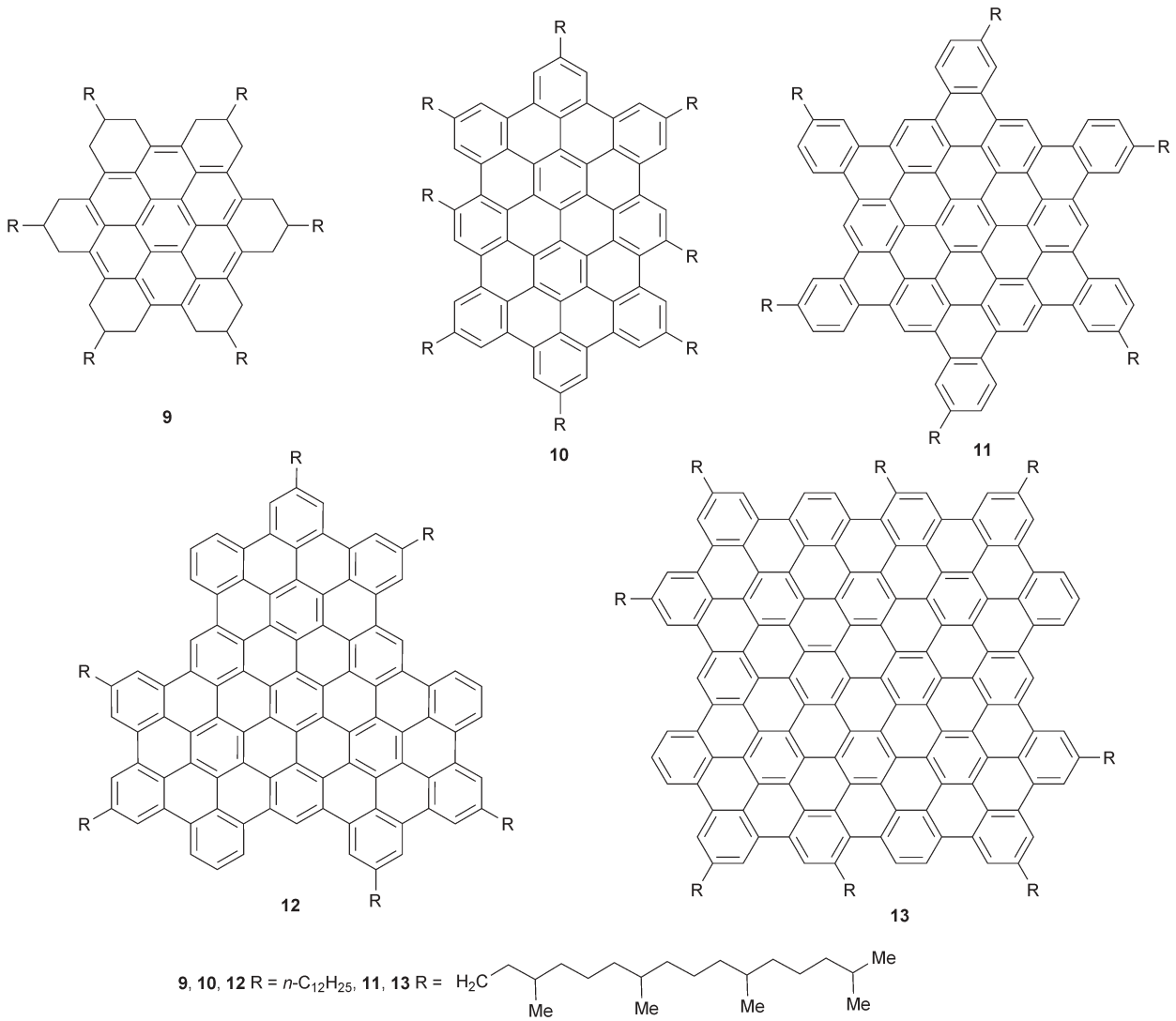

Fig. 4 Chemical structures of disc-like PAHs of various diameters (d_{core}): **9** (*ca.* 1.0 nm), **10** (*ca.* 1.6 nm), **11** (*ca.* 1.9 nm), **12** (*ca.* 2.0 nm), **13** (*ca.* 2.3 nm). For comparison, **1**, **3** and **7** depicted in Fig. 3 have core diameters of *ca.* 0.8 nm, *ca.* 1.9 nm, and *ca.* 1.4 nm, respectively.

Table 1 Charge carrier mobility values and maxima of the first absorption band of PAH **7** and **9–13**

PAH molecule	Number of aromatic C atoms in the core	λ_{max}/nm[54]	$\Sigma\mu_{1D}$ in the columnar LC phase/cm^2 V^{-1} s^{-1}	
			Found[54]	Calculated[54]
9	24	331	0.1–0.2	0.09
7	42	361	0.38	0.42
10	60	410	0.26	0.75
11	78	430	Not measured[a]	
12	96	462	0.20	1.26
13	132	546	Not measured[a]	

[a] Conductivity of these samples saturates within the pulse and then rapidly decreases to the noise level.

that could be expected for an aromatic core of infinite size ($1/n = 0$).[55]

The experimentally found and calculated values for HBC **7** and PAHs **9–13** (R = alkyl, see Fig. 3, 4) are given in Table 1. For the relatively small **7** and **9**, the results of PR-TRMC measurements are in good agreement with calculations. Moreover, there is a drastic increase in mobility over yet smaller triphenylene derivatives (average μ values between 0.002 and 0.025 cm^2 V^{-1} s^{-1}).[55] However, for aromatic cores with 60 or more carbon atoms the measured values are not supported by the calculation results and instead remain rather insensitive to the core size. One reason for this could be the influence of fluctuations within columnar stacks on the charge transfer integral, as discussed in recent theoretical works.[42,56,57]

Another important issue that should be raised here is the purity of the compounds. Notably, thorough purification of **11** and **13** was not feasible because of their extremely poor solubility in all common organic solvents.[54] At the same time, conductivity of these samples saturates within the pulse and then rapidly falls to the noise level, making the mobility measurements impossible. This could be due to the sensitivity of the conductivity towards traces of inorganic impurities acting as charge traps. In fact, a charge carrier with a mobility of *ca.* 1 cm^2 V^{-1} s^{-1} would visit *ca.* 200 molecular sites within one nanosecond. This means that the presence of

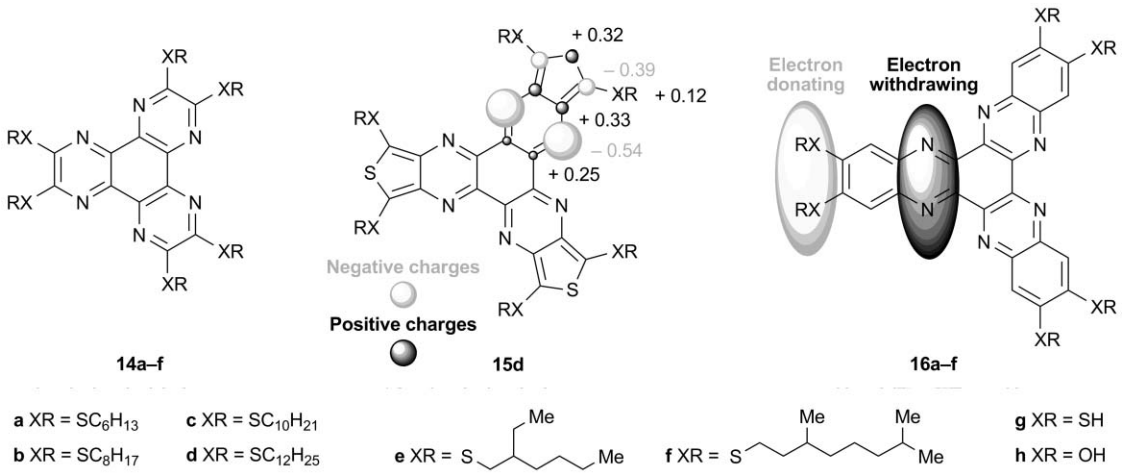

Fig. 5 Molecular structures of hexaazatriphenylenes (HAT) **14a–f**, hexaazatriisothianaphthene **15d** and hexaazatrinaphthylenes (HATNA) **16a–h**. The charge distribution of **15g** has been calculated.[58] The size of the shaded spheres is proportional to the partial charge on each atom; light grey and dark grey spheres correspond to negative and positive charges, respectively.

charge-trapping impurities even in small amounts will be detrimental to the charge transport.[54]

Besides the charge transport properties of discotic materials, their optical properties are also important in view of potential applications in photovoltaic cells or LEDs (see also Section 4). For such applications, high absorption coefficients over a large range of wavelengths are desirable. Enlargement of the aromatic core of PAH represents an excellent means of achieving this objective. Indeed, with increasing size of aromatic cores the absorption maximum shifts from 331 nm for **9** to 546 nm for **13**. The values of λ_{max} follow the empirical linear relationship $\lambda_{max} = 280 + 2n$, where n is a number of C atoms in the aromatic core. Furthermore, the bathochromic shift is accompanied by essential broadening of absorption bands.[54]

2.2. Shape of wavefunctions

From the above discussion it is obvious that although size does matter, it is not the only factor that influences charge transport. The interplay of the structure of the conjugated core with the connecting groups of the side chains must be further discussed within the concept of *the shape of the wavefunctions*. Fig. 5 depicts three classes of disc-shaped molecules **14**, **15** and **16** that share the following structural elements: (i) six nitrogen atoms located in the center of the molecule, and (ii) six or nine sulfur atoms at the periphery of the conjugated core.

This specific design of donor and acceptor groups has been devised to locate the HOMO (LUMO) in the center of the molecules in the hope of increasing the orbital overlap and finally improving the hole (electron) transport. The idea was also to design robust systems that would have little variation of orbital splitting upon rotation of disc-like molecules around their director axis since in columnar stacks.[59,60] Fig. 6 (left) shows the LUMO of hexaazatrinaphthylene (HATNA) **16g**. The largest LCAO coefficients are calculated on the nitrogen atoms in the center of the molecule. As a result of the shape of the wavefunction, the splitting of the LUMO varies from approximately 0.4 to 1.5 eV for rotation angles of adjacent

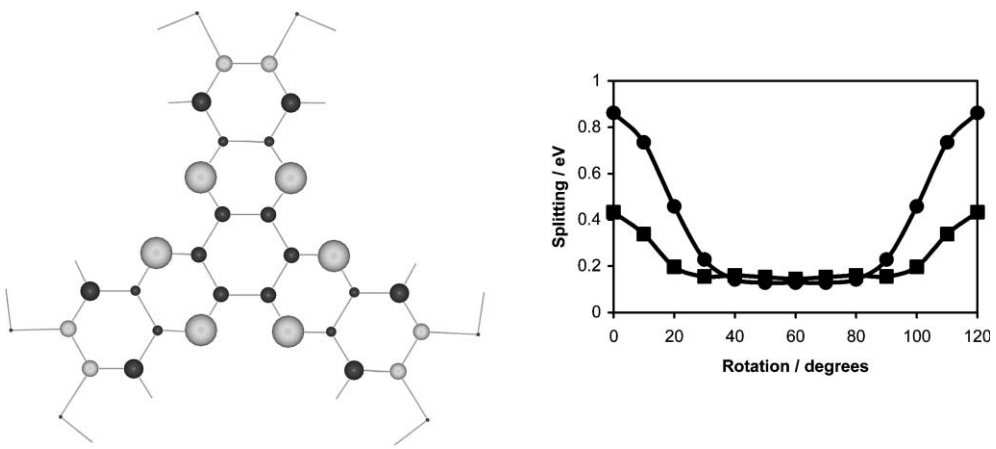

Fig. 6 Left: shape of the LUMO of **16g**. The shade and the size of the spheres correspond to the sign and the amplitude of the LCAO coefficients, respectively. Right: INDO-calculated evolution of the HOMO (circles) and LUMO (squares) splittings in a cofacial dimer made of two HATNA (**16**) molecules as a function of the rotational angle between the discs.

molecules from 0° (eclipsed conformation) to 60° (staggered conformation), respectively. It could be concluded from the above discussion that the presence of the six nitrogen atoms in **14**, **15** and **16** brings only advantages. This is however not true, since partial negative charges that can be as high as $-0.54|e|$ are present on each of them. The consequence is that no LC mesophase is observed for **14a–f**[61] and **15d** due to electrostatic repulsion between partial negative charges.[58] In the case of **16a–e**, which form columnar mesophases over a large temperature range, this electrostatic repulsion is compensated by more efficient π-stacking of the larger HATNA core. These mesogens exhibit, however, very little intracolumnar order in LC phases, *i.e.* the discs are not positioned at a regular distance within the columns. Nevertheless, μ values measured by the PR-TRMC technique for **16b–d** range from 0.02 to 0.2 $cm^2\ V^{-1}\ s^{-1}$.[62]

The most spectacular effects of ordering on electronic properties are observed for **16a** which shows poor PR-TRMC μ values (below 0.01 $cm^2\ V^{-1}\ s^{-1}$) even in its room temperature crystalline phase. Ultraviolet photoelectron spectroscopy (UPS) has been used to record the ionization potential (IP) of **16a**. A constant value of 5.9 eV has been measured for pristine spin-coated films on various substrates. Upon thermal annealing the films of **16a** (columnar hexagonal phase) become more ordered. The IP measured at room temperature after this thermal treatment has shifted to 4.1 eV, *i.e.* 1.8 eV lower than in the disordered films before annealing![19] The bandwidth of the HOMO is estimated to be 1.1 ± 0.2 eV. This experimental value has the same order of magnitude as the interplanar bandwidth in graphite (1.0–1.4 eV) and is much larger than those estimated in molecular crystals (*ca.* 0.5 eV for oligoacenes).[19] These observations have been rationalized by quantum-chemical calculations performed on model stacks containing from two to six molecules, which illustrate the formation of a quasi-band structure with Bloch-like orbitals delocalized over several molecules in the column.[19] Independently of the experimental work on **16a**, a theoretical model which takes into account the delocalization of charges over a few stacked molecules has been suggested.[63] It is hypothesized that the packing of **16a** in bulk and in thin films should be different to explain the apparent discrepancy between the low μ observed in bulk and the quasi-band like behavior observed in thin films.

In summary, the chemical structure and the diameter of the conjugated core of discotic LCs govern, to a large extent, their electronic properties at the molecular level. Clear-cut structure–property relationships are however not directly accessible, since supramolecular order, which depends in a subtle and non predictable manner on chemical structure, dramatically influences electronic properties of materials. In the next section, the role of connecting groups between a conjugated core and flexible side chains will be discussed.

2.3. Connecting groups

The connecting groups between the aromatic core and the flexible peripheral substituents (often alkyl chains) play a twofold role. On the one hand, they substantially modify the supramolecular order. This is evidenced by the thermotropic behavior of mesogens, as illustrated by octa-substituted phthalocyanines (**3–6**, Fig. 3 and Table 3, below). In some special cases, when connecting groups are involved in specific non-covalent intermolecular interactions, this effect is particularly striking. An example worth mentioning is the hexaamide derivative of triphenylene **17** (Fig. 7) which exhibits an inter-disc distance as short as 3.18 Å, *i.e.* much smaller than the sum of the van der Waals radii of carbon atoms in PAHs, due to the efficient intermolecular H-bonding.[64] Supramolecular organization of discotic LC is discussed in detail below (see Section 3).

Table 2 Internal reorganization energy for positive (λ_{i+}) and negative (λ_{i-}) polarons of selected conjugated core with and without substituents

Core	Molecule[a]	λ_{i+}/meV	λ_{i-}/meV	Ref.
Triphenylene	**1**, XR = H	180	260	42
Triphenylene	**1**, XR = SH	160	240	42
Triphenylene	**2**, XR = OH	330	400	42
Pc	**3**, XR = H	47	225	6
HBC	**7**, XR = H	100	140	42
HATNA	**16**, XR = H	140	100	42
HATNA	**16g**	100	110	42
HATNA	**16h**	380	490	42
Pentacene		97	132	65

[a] See Fig. 3 and Fig. 5 for molecular structures.

On the other hand, the connecting group dramatically influences the reorganization energy in the Marcus equation. Table 2 collects the internal reorganization energy for positive (λ_{i+}) and negative (λ_{i-}) polarons of selected conjugated cores with and without substituents. It is observed that oxygen atoms dramatically increase both λ_{i+} and λ_{i-}, whereas sulfur atoms have only a marginal influence. However, this general

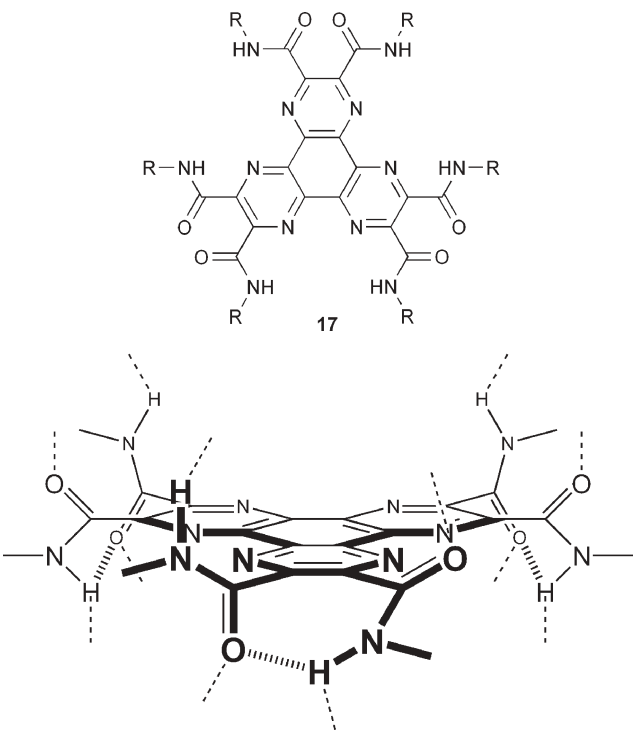

Fig. 7 Molecular structure of the hexaamide derivative of triphenylene **17** which exhibits an inter-disc distance as short as 3.18 Å.

Table 3 Transition temperatures and phase behavior of selected discotic mesogens

	Connecting group	Side chains	Phase behavior (transition temperatures/°C)[a,b]	Ref.
1a	S	*n*-C_6H_{13}	Cr 62 Col_{ho} 70 Col_{hd} 93 I	68
2a	O	*n*-C_6H_{13}	Cr 68 Col_h 97 I	69
3b	O	*n*-C_8H_{17}	Cr 94 Col_h > 350 (dec)	43
3c	O	*n*-$C_{10}H_{21}$	Cr 94 Col_h 345 I	43
3d	O	*n*-$C_{12}H_{25}$	Cr 83 Col_h 309 I	43
3e	O	*n*-$C_{18}H_{37}$	Cr 98 Col_h 247 I	70
4d	CH_2	*n*-$C_{11}H_{23}$	Cr 120 Col_h 252°	44
5d	CH_2O	*n*-$C_{12}H_{25}$	Cr 79° Col_x 185° Col_h 260°	45
6d	COO	*n*-$C_{12}H_{25}$	Cr 62° Col_h > 300°	47
7	CH_2	*n*-$C_{11}H_{23}$	Cr 107° Col_h 417°	71
8	*p*-Phenylene	*n*-$C_{12}H_{25}$	Col_{x1} 18 Col_{x2} 83 Col_{x3}	72
14a	S	*n*-C_6H_{13}	Cr 105 I	61
15d	S	*n*-$C_{12}H_{25}$	Cr 59 I	58
16a	S	*n*-C_6H_{13}	Cr 206 > 250 (dec)	62
16b	S	*n*-C_8H_{17}	Cr 178 Col_{hd} > 250 (dec)	62
16c	S	*n*-$C_{10}H_{21}$	Cr 116 X 134 Col_{rd} > 250 (dec)	62
16d	S	*n*-$C_{12}H_{25}$	Cr 99 Col_{rd} > 250 (dec)	62
16e	S	2-Et-C_6H_{13}	Cr > 250 (dec)	73
16f	S	3,7-diMe-C_8H_{17}	Cr 206 Col_x > 250 (dec)	73
17	CONH	*n*-$C_{12}H_{25}$	Col_x > 250 (dec)	64
18a	O	2-Et-C_6H_{13}	<−20 Col_h > 260 (dec)	74
18b	O	2-(*n*-Bu)-C_8H_{17}	<−20 Col_r 79 Col_h > 250 (dec)	75
18c	O	2-(*n*-C_6H_{13})-$C_{10}H_{21}$	<−20 Col_r 91 Col_h > 250 (dec)	75
18d	O	2-(*n*-C_8H_{17})-$C_{12}H_{25}$	<−20 Col_r 68 Col_h 226 I	6
18e	O	2-(*n*-$C_{10}H_{21}$)-$C_{14}H_{29}$	<−20 Col_r 60 Col_h 180 I	6
19a	CH_2	2-Et-C_6H_{13}	Cr 97 Col_d 420 I	76
19c	CH_2	2-(*n*-C_6H_{13})-$C_{10}H_{21}$	Col_p 17 Col_d 97 I	76
19e	CH_2	2-(*n*-$C_{10}H_{21}$)-$C_{14}H_{29}$	Col_p 46 I	76,77
20b	COO	2-(*n*-Bu)-C_8H_{17}	Col_r 149 I	47
20c	COO	2-(*n*-C_6H_{13})-$C_{10}H_{21}$	<25 I	47
21	O	$(CH_2CH_2O)_3Me$	19 Col_{ho} 293 I	78

[a] Phases: Cr crystalline, Col_p columnar plastic crystalline, Col_h columnar hexagonal, Col_{hd} columnar hexagonal disordered, Col_r columnar rectangular, Col_{rd} columnar rectangular disordered, Col_d columnar disordered, Col_x columnar unspecified, I isotropic, X unidentified. [b] Multiple crystalline phases are not shown.

tendency is modulated by an additional element, the orbital coefficient on the carbon atom of the π-system directly connected to the heteroatom.[6]

Let's now turn to the combined influence of connecting group and side chains on the phase behavior of discotic molecules.

2.4. Phase behavior and transition temperature engineering

From a fundamental viewpoint, supramolecular order in mesophases is the most important parameter for efficient charge transport. However, in order to transfer the advantages of LC semiconductors into device applications, other conditions should be fulfilled as well. Necessarily, the potential candidates should be well-soluble in organic solvents to allow easy processing by spin coating or other solution methods. On the other hand, processing of the material by thermal annealing requires reasonably low clearing points: the upper temperature limit for fabrication of devices on flexible plastic substrates is often considered to be *ca.* 200 °C.[66] Further, the materials should be liquid crystalline at the ambient temperature and LC mesophases should be stable over a sufficiently broad temperature range. Tuning of the thermotropic behavior thus appears to be another crucial issue in the design of discotic mesogens.

The simplest approach to controlling the temperature of the transition between the crystalline (Cr) and LC phases (melting point) or between LC phases and the isotropic liquid (clearing point) comprises variation of the length of peripheral substituents, most typically alkyl chains. As an example, studies of octa(*n*-alkoxy) and octa(*n*-alkyl) phthalocyanines **3** and **4** clearly revealed the influence of side chain length in these homologous series of discotic molecules. Elongation of substituents lowers the clearing points in both series of phthalocyanines. Moreover, a close to linear dependence between the clearing points and the number of carbon atoms in the alkyl side chains was observed for both **3** and **4**. The temperatures of Cr–LC transitions generally decrease with increasing chain length until reaching a minimum and subsequently increase again, reflecting the crystallization tendency of the linear alkyl side chains (see **3b–e**, Table 3).[27,43,44,67] Thus, simply changing the length of alkyl chains is not always efficient enough for the tuning of the transition temperature, and in particular, room temperature LC phases are difficult to achieve.

Formation of discotic mesophases can often be satisfactorily described by a simple model involving separate disordering temperatures for the side chains and the aromatic cores. The transition between crystalline (Cr) and LC phases involves the conformational disordering of side chains, also referred to as "side chain melting", while aromatic cores remained stacked until reaching the isotropization temperature.[79] According to this model, branching of the side chains of discotic molecules should decrease Cr–LC transition temperatures. Indeed, branching should make the regular packing of side chains

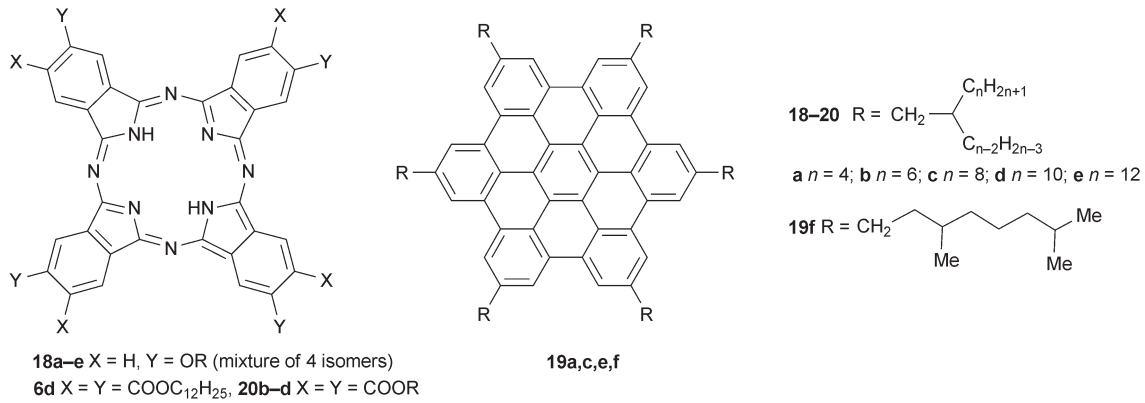

Fig. 8 Chemical structures of phthalocyanines **18a–e** and **20b–d** bearing four alkoxy or eight alkoxycarbonyl branched side chains, respectively, and HBC **19a,c,e,f** bearing six branched alkyl side chains.

more difficult, promote kinking (*gauche* conformations) and, in the case of racemic chiral side chains, also introduce stereoheterogeneity. On the other hand, when the branched substituents are sufficiently bulky, their steric repulsion should also affect stacking of the aromatic cores and reduce the isotropization temperatures. Both effects were demonstrated for the hexaalkyl-HBC series of discotic mesogens (Fig. 8). While short-chain **19a** is crystalline at room temperature, forms mesophases only above *ca.* 100 °C and has a very high clearing point (*ca.* 420°), **19c** with longer and more sterically demanding substituents is liquid crystalline at room temperature and its clearing point is lowered by more than 300 °C compared to **19a**.[76] In the same way, octaalkoxycarbonyl phthalocyanine **20b** bearing eight branched 2-butyloctyl substituents has a clearing point of 150 °C while its straight-chain analog **6d** remains liquid crystalline even at 300 °C. Further elongation of the branched chains to 2-hexyldecyl gave **20c** which is liquid at room temperature.[47] A similar behavior was observed for the family of tetraalkoxy phthalocyanines **18a–e** (see also Table 3).[6,74] However, the decrease of isotropization temperature with the increasing length of the branched substituent was less pronounced. This is certainly due to the smaller number of alkyl chains and their less dense packing on the periphery of the phthalocyanine core in the tetra-substituted derivative. The use of branched alkyl chains has proved fruitful to reduce transition temperatures of many structurally different discotic molecules.[80]

It clearly appears from the previous discussion that the steric hindrance introduced by branching of the side chains has an important influence on the phase behavior of discotic mesogens. However, the role of stereoheterogeneity of discotic materials is not negligible, either, as demonstrated for the HBC derivative **19f**. The temperature of Cr–LC transition for the stereohomogeneous (all-*S*)-**19f** is 15 °C higher than that of **19f** bearing racemic side chains and comprising multiple diastereoisomers.[81]

Alkyl side chains are most frequently used in the design of discotic mesogens due to the availability of the broad range of the corresponding starting materials (alcohols or alkyl halides). However, other types of peripheral substituents have been successfully explored. Thus, oligo(ethyleneoxy) chains efficiently induce mesogenicity of Pc derivatives. Interestingly, both the temperature of Cr–LC transition and the clearing point of octa-substituted Pc **21** bearing eight oligoether side chains are notably lower (by 75 and 52 °C, respectively) than those of the octadecyloxy analog **3c** that differs only in the nature, and not in the length, of the peripheral substituents.[43,78] The stabilization of mesophases by oligoether chains may be explained by their greater flexibility compared to alkyl chains that enhance the disc-shape anisotropy.

An interesting and relatively recent concept in the design of discotic semiconductors is the use of polyfluorinated alkyl chains. These substituents are expected to create a fluorinated "mantle" around the discotic core that should greatly reduce the intercolumnar interactions and hence improve the one-dimensional charge carrier transport. A few years after early studies on polyfluoroalkyl triphenylenes,[85] it was shown that introduction of polyfluoroalkyl groups generally favors the formation of homeotropic alignment[86] (see Section 3 for a detailed discussion about alignment of discotic mesogens). In addition, triphenylene derivatives **22** (Fig. 3) with relatively high fluorine content form mesophases with a wider temperature range compared to their hexaalkoxy analogs **2** (Table 4).[82,83] Recently, a series of HBC derivatives **23** (Fig. 3) bearing six perfluoroalkyl chains separated from the aromatic core by either oligomethylene or *p*-phenylene spacers has been reported. Derivatives with $(CH_2)_n$ spacers do form discotic mesophases with a broad temperature range, but

Table 4 Fluorinated discotic mesogens and their alkyl analogs

	Aromatic core	Side chain	Phase behavior[a,b]	Ref.
2a	Triphenylene	n-C_6H_{13}	Cr 67 Col_h 99 I	82, 83
22a	Triphenylene	$(CH_2)_3(CF_2)_2CF_3$	Cr 130 Col_h 149 I	82, 83
2b	Triphenylene	n-C_7H_{15}	Cr 64 Col_h 89 I	82, 83
22b	Triphenylene	$(CH_2)_3(CF_2)_3CF_3$	Cr 116 Col_h 157 I	82, 83
2d	Triphenylene	n-C_9H_{19}	Cr 56 Col_h 77 I	82, 83
22c	Triphenylene	$(CH_2)_3(CF_2)_5CF_3$	Cr 89 Col_h 183 I	82, 83
23a	HBC	$(CH_2)_2(CF_2)_7CF_3$	Cr 180 Col_r> 300 (dec)	84
23b	HBC	$(CH_2)_4(CF_2)_7CF_3$	Cr 120 Col_h > 300 (dec)	84
23c	HBC	$(CH_2)_6(CF_2)_5CF_3$	Cr 109 Col_h > 300 (dec)	84

[a] Phases: Cr crystalline, Col_h columnar hexagonal, Col_r columnar rectangular, I isotropic. [b] Multiple crystalline phases are not shown.

decompose above 300 °C before reaching the isotropization point.[84] In both triphenylene and HBC series of mesogens with partly fluorinated alkyl chains, the isotropization temperatures increase with increasing fluorine content (Table 4).

Another appealing concept consists in the substitution of the aromatic core with sufficiently bulky substituents, *e.g.* arylethynyl groups, resulting in star-shaped discotic mesogens. Thus, pyrene derivative **24** bearing twelve dodecyl chains (Fig. 9) forms columnar LC phases and exhibits a high fluorescence quantum yield in the solid state.[25] The steric hindrance caused by the bulky connecting groups and side chains forces adjacent molecules to pack with their transition dipoles non-parallel.

Star-shaped hexa(alkyl)phenyl HBC **8** brings about the following advantage over the hexaalkyl analog **7** (see Fig. 4): better solubility, longer range order in the mesophase and an outstanding charge carrier mobility.[72,87] Extending this concept, the star-shaped discotics **27a–d**, **28** and **29** were synthesized *via* Sonogashira–Hagihara coupling of the hexaiodo precursors **25** and **26** (Scheme 1). All star-shaped HBC derivatives **27a–d** and **28** have thermally stable mesophases and no clearing points below 400 °C.[88,89] The hexa(alkylethynyl) derivative **27a** shows a similar phase behavior to the alkylaryl derivative **8**. In contrast, **27b** and **27c** demonstrate more complex phase behavior, presumably due to the increasing volume of the terminal substituents.[90] Further, triarylamine substituents were introduced (**27d** and **28**) to realize the concept of a molecular double cable: columnar stacking would produce two charge transport pathways, one along the HBC columns and another along the amine stacks on the outer side of the columns. Although the hexaamine substituted HBC **27d** and **28** did not show any phase

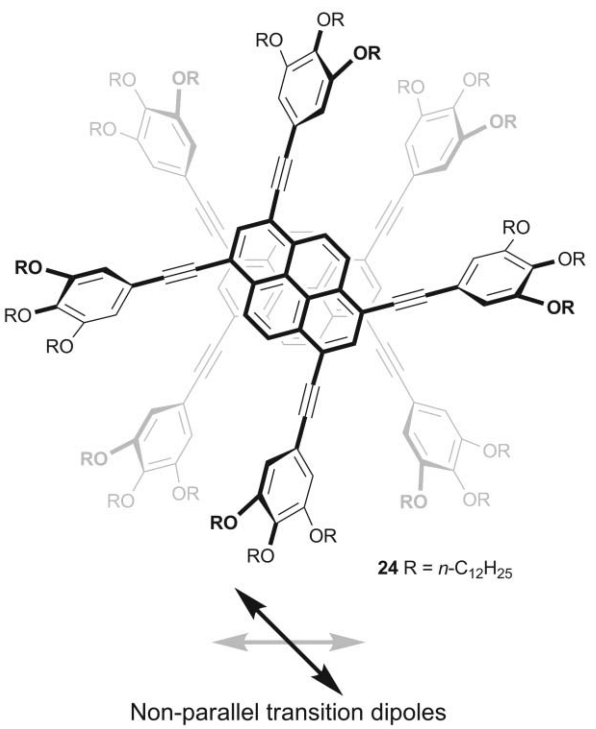

Fig. 9 Molecular structure of star-like pyrene derivative **24**.

transitions between −100 °C and 400 °C, two-dimensional wide-angle X-ray scattering (WAXS) experiments on extruded fibers clearly revealed the columnar hexagonal phases. At the same time, the measured charge carrier mobility (0.04 and 0.03 $cm^2 V^{-1} s^{-1}$ for **27d** and **28**, respectively) was much lower than in the hexaalkyl HBC, probably due to a lower degree of order in these materials.[91]

A water-soluble star-shaped HBC derivative **29** bearing eighteen oligoether chains has a dramatically reduced clearing point compared to *n*-alkyl-substituted HBCs (Col_h phase between room temperature and 150 °C). ^1H NMR in chlorinated solvents confirmed the existence of only monomeric **29**, but in protic polar solvents (water, methanol) **29** is strongly aggregated due to hydrophobic interactions.[92] Amphiphilic star-shaped HBCs **30a,b** bearing branched oligoethers have been prepared by direct cyclotrimerization of the corresponding diarylethynes followed by oxidative cyclization ($FeCl_3$ in $MeNO_2$); they form a discotic columnar mesophase between room temperature and 350 °C (decomposition temperature).[93]

2.5. Low-symmetry discotic molecules

For synthetic reasons, most known discotic molecules comprise highly symmetrical aromatic cores decorated with identical peripheral substituents. However, discotic molecules with lower symmetry, though more synthetically challenging, offer additional opportunities for the tuning of properties and supramolecular organization. In general, lower symmetry should entropically disfavor crystallization and hence, stabilize the mesophases. One may distinguish between the following possibilities in the design of less-symmetrical discotics: (i) changing the *substitution pattern* of the same highly symmetrical core; (ii) building up aromatic disc-like molecules with *lower inherent symmetry* but bearing all identical substituents; (iii) binding two or more rigid cores by appropriate spacers into "*discotic dimers or oligomers*".

2.5.1. Variation of substitution pattern. Assembly of discotic cores by the cyclooligomerization of smaller precursors necessarily provides fully symmetrical molecules. Typical examples are HBCs, phthalocyanines (Pc) and triphenylenes, possessing six-, four- or three-fold rotational symmetry, respectively. They are prepared *via* the metal-catalyzed trimerization of symmetrical diarylacetylenes, base-promoted tetramerization of 4,5-disubstituted-1,2-benzodinitriles and oxidative trimerization of 1,2-disubstituted benzenes, respectively. If a mixture of two (or more) precursors with different substituents is subjected to the cyclization, it necessarily leads to complex mixtures of products. This method of synthesis can only be practical when a difference in polarity ensures the reasonably facile separation of products. Examples of such "statistical" approaches to some unsymmetrically substituted Pc and triphenylenes have been reviewed earlier.[29] Here we will mention only the recently prepared heptaethynyl substituted C_s-symmetrical Ni-Pc that forms an unusual columnar phase where each "super-disc" in the column is formed by the two Pc units.[94]

The advantages of the "rational" approach that would yield discotic molecules with precisely defined composition and

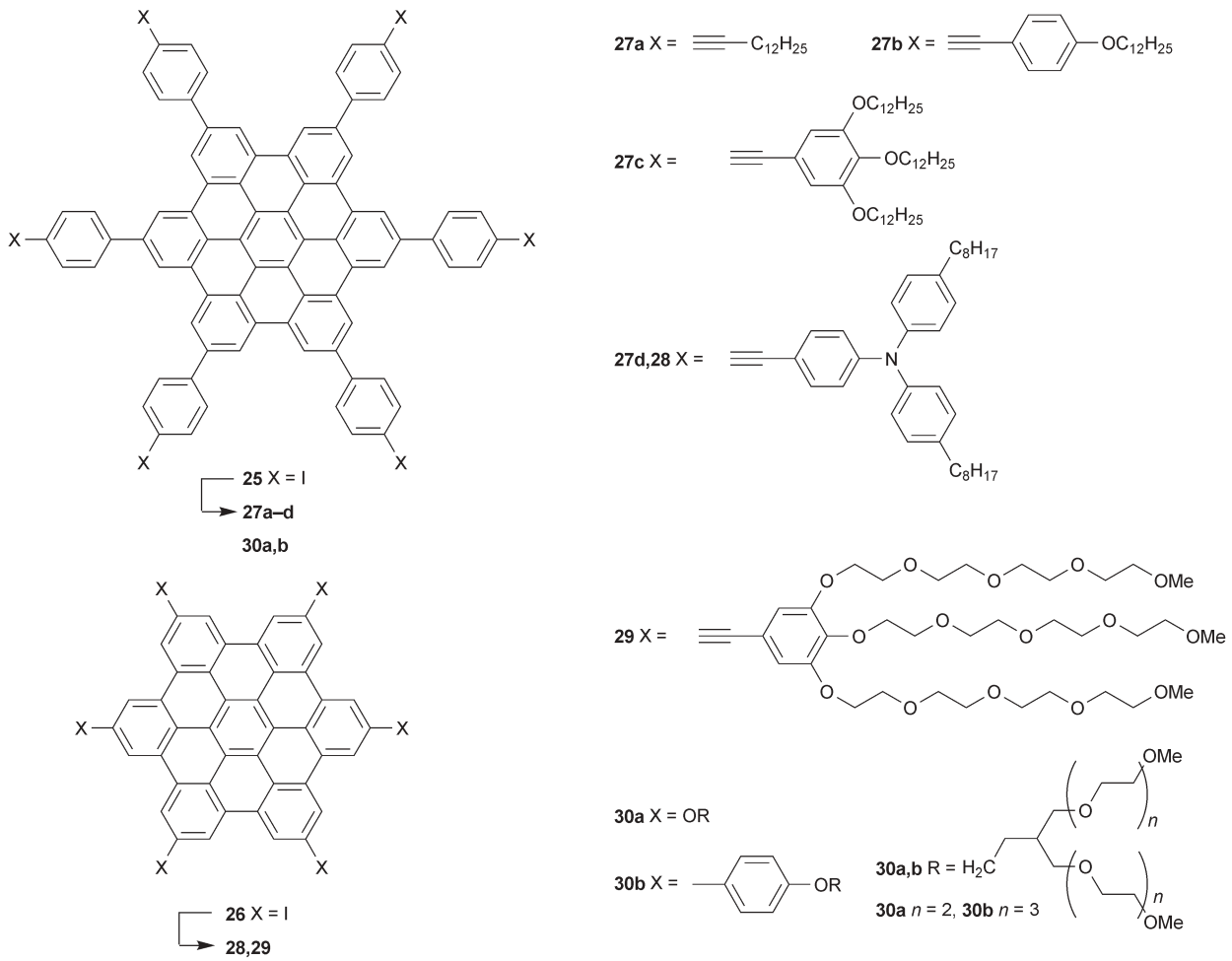

Scheme 1 Star-shaped HBC derivatives.

structure over the "statistical" approach, resulting in the mixtures of products, are quite evident. Rational strategies for the synthesis of triphenylenes have recently been presented in a tutorial review.[95] Thus, only selected examples not covered by this review will be discussed below. An elegant and at the same time rather simple "rational" approach to lower-symmetry discotics relies on the "extra" substitution of the highly symmetrical aromatic core *via*, *e.g.*, an electrophilic substitution. Nitration of hexaalkoxytriphenylene **2a** yields the nitro derivative **31** that is liquid crystalline at room temperature and has a much broader mesophase range compared to **2a** (Table 5). In addition, the nitro group can be easily converted into a number of other functionalities (amino, azido, alkylamido) and some of them also demonstrate enhanced

Table 5 Low-symmetry discotics (**2a** and **7** are given for the sake of comparison)

	Overall symmetry of molecule	Aromatic core	Number and structure of side chains	Phase behavior	Ref.
2a	D_{3h}	Triphenylene	6 OC_6H_{13}	Cr 68 Col_h 97 I	69
31	C_s	Triphenylene	6 OC_6H_{13}	Col_x 136 I	96
34	D_{3h}	Triphenylene	6 $COOC_6H_{13}$	Cr 108 Col_r 120 I	29
33a	C_s	Triphenylene	4 COOEt	Cr 70 Col_h 218 I	98
33b	C_s	Triphenylene	4 $COOC_6H_{13}$	Cr 58 Col_h 91 I	98
33c	C_s	Triphenylene	4 COO(2-Et-C_6H_{13})	Col_h 121 I	98
39	C_{2v}	HBC	4 *n*-$C_{12}H_{25}$	Cr 59 Col_{ho} > 420 I	99
41	D_{2h}	HBC	4 *n*-$C_{12}H_{25}$	Cr 104 Col_{ho} > 420 I	99
7	D_{6h}	HBC	6 *n*-$C_{12}H_{25}$	Cr 107 Col_h 420 I	71
38	C_{2v}	HBC	5 *n*-$C_{12}H_{25}$	Cr 124 Col_{ho} 412 I	99
40	C_{2v}	HBC	4 *n*-$C_{12}H_{25}$	Cr 147 Col_{ho} 400 I	100, 108
48	C_{2v}	HBC-analog	4 *n*-$C_{12}H_{25}$	Cr 148 Col_{ho} 420 I	108
49	C_{2v}	HBC-analog	4 *n*-$C_{12}H_{25}$	Cr 173 Col_{co} 210 I	108
50	D_{3h}	HBC-analog	6 *n*-$C_{12}H_{25}$	Cr 48 Col_{ho} > 500 I	108

[a] Phases: Cr crystalline, Col_h columnar hexagonal, Col_{ho} columnar hexagonal ordered, Col_{co} columnar cubic ordered, Col_r columnar rectangular, Col_r columnar unspecified, I isotropic. [b] Multiple crystalline phases are not shown.

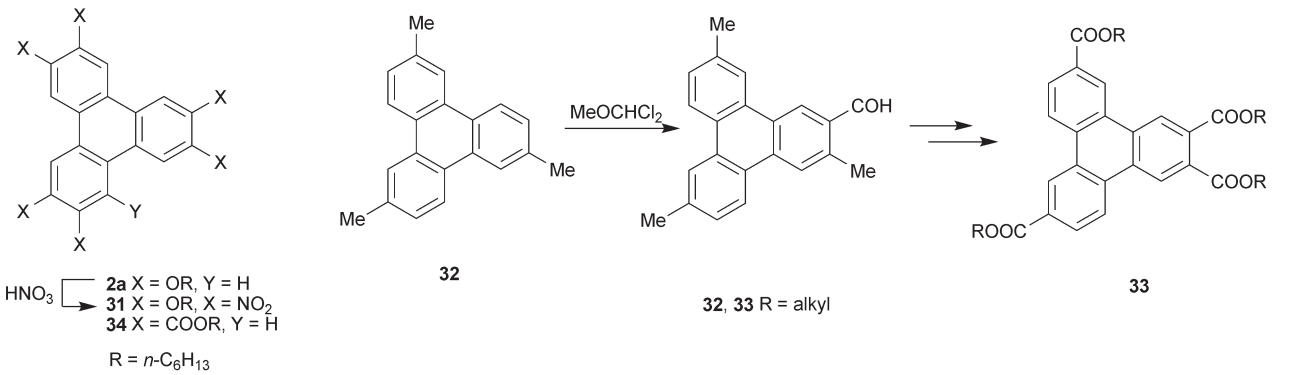

Scheme 2 Synthesis of triphenylene derivatives lacking rotational symmetry.

mesophase properties.[96] Heptasubstituted triphenylenes with "extra" alkoxy substituents have been prepared from highly symmetrical hexaalkoxytriphenylenes **2** *via* three-step synthesis.[97]

Triphenylenes **33** bearing four alkoxycarbonyl groups and lacking rotational symmetry have been prepared *via* the regioselective formylation of 2,6,10-trimethylphenylene (**32**) in a key step (Scheme 2). Even when alkyl chains are as short as ethyl, tetraesters **33** are liquid crystalline at or close to room temperature. Columnar mesophases of tetraesters **33** are stable over a much broader range than those of the highly symmetrical hexaesters with identical substituents (compare **33b** and **34**, Table 5 and Scheme 2) and in addition, form homeotropically aligned films.[98]

In spite of the appealing simplicity of the desymmetrization approach described above, chemists sometimes choose longer and more challenging synthetic routes towards lower-symmetry discotics. As an example, the synthesis of low-symmetry HBC derivatives will be considered. Cyclotrimerization of symmetrical di(alkylaryl)acetylenes followed by the oxidative cyclization of the hexaarylphenyl intermediate necessarily leads to the D_{6h}-symmetrical hexaalkyl HBCs such as **7** (Fig. 3). However, a Diels–Alder cycloaddition between diarylacetylenes **35** and tetraarylpentacyclodienones **36** with a properly chosen combination of substituents (see Scheme 3 for representative examples) gives access to penta- or tetraalkyl derivatives as single reaction products.[99,100] These substitution patterns can be termed "*mono*", "*ortho*" and "*para*" by analogy with benzene derivatives, as HBC can be considered as a "superbenzene".

Notably, this approach provides the bromo and iodo HBC derivatives **37**, **39** and **41**. A "1,3,5-trisubstituted" triiodo derivative of HBC bearing three alkyl chains was prepared *via* an alternative synthetic route.[91] These valuable intermediates can easily be converted *via* metal-catalyzed cross coupling reactions into a number of useful functional derivatives (Scheme 3) as well as to complex molecules containing more than one HBC core (see below).[99] Among the other molecules, diarylamino derivatives **42** and **43** have been prepared from **37** and **39**, respectively, by the Buchwald–Hartwig coupling in order to provide another entry to the "molecular double cable" concept (see above). Unlike the star-shaped HBCs **27d** and **28**, the diarylamine-substituted derivatives **42** and **43** do form liquid crystalline mesophases above 217 °C and 162 °C, respectively. Moreover, they exhibit relatively high charge carrier mobilities (0.11 and 0.21 $cm^2\ V^{-1}\ s^{-1}$, respectively). Whether these values reflect more efficient hole transport along the ordered amine stacks compared to disordered solid phases, or a comparable mobility of electrons that remain localized in the HBC cores with that of holes on the amine units, remains unanswered. The PR-TRMC method is insensitive to the sign of charge carriers and cannot therefore distinguish between these two possibilities (various experimental methods for the measurement of charge carrier mobility will be discussed below, see Section 4).[90]

Synthetic routes to low-symmetry HBC and triphenylene derivatives pave the way to donor–acceptor discotic dyads such as **44–46** (Scheme 3).[101–104] The interest in such elaborate molecular structures is twofold. First, the bulky side groups considerably modify the supramolecular order, and second, they constitute unique systems for photovoltaic applications. The distance between a donor and an acceptor moiety, and as a consequence, the kinetics of electron transfer can be tailored from the synthesis. Rapid hole or electron transport along donor or acceptor columnar stacks, respectively, is anticipated.

Finally, an interesting amphiphilic HBC derivative **47** bearing two alkyl and two oligoether chains attached to the aromatic core (Fig. 10) has been prepared *via* the same general strategy as shown in Scheme 3. This design prevents the columnar self-assembly typically encountered for HBC derivatives. Instead, in THF **47** self-assembles into bilayer tapes due to interdigitation of the alkyl chains of π-stacked discs. Rolling-up of this tape produces hollow tubular objects with a length greater than 10 μm and an internal diameter of *ca.* 14 nm, that is, an order of magnitude larger than carbon nanotubes. Both internal and external surfaces of the nanotube composed of *ca.* 50 000 disc-like molecules are covered by hydrophilic triethyleneglycol chains that suppress formation of multilayer structures in polar solvents such as THF.[105] Very recently, nanotubes with one-handed helical chirality have been fabricated *via* the introduction of a stereogenic center into each of the oligoether chains.[106] This chiral nanotubes form macroscopic fibers with anisotropic electrical conduction.[107]

2.5.2. Variation of the aromatic core. Very recently, the synthesis of "HBC-like" PAHs with "zigzag" peripheries possessing lower inherent symmetry of aromatic cores compared to the pristine HBC was described (Fig. 11).[108] A

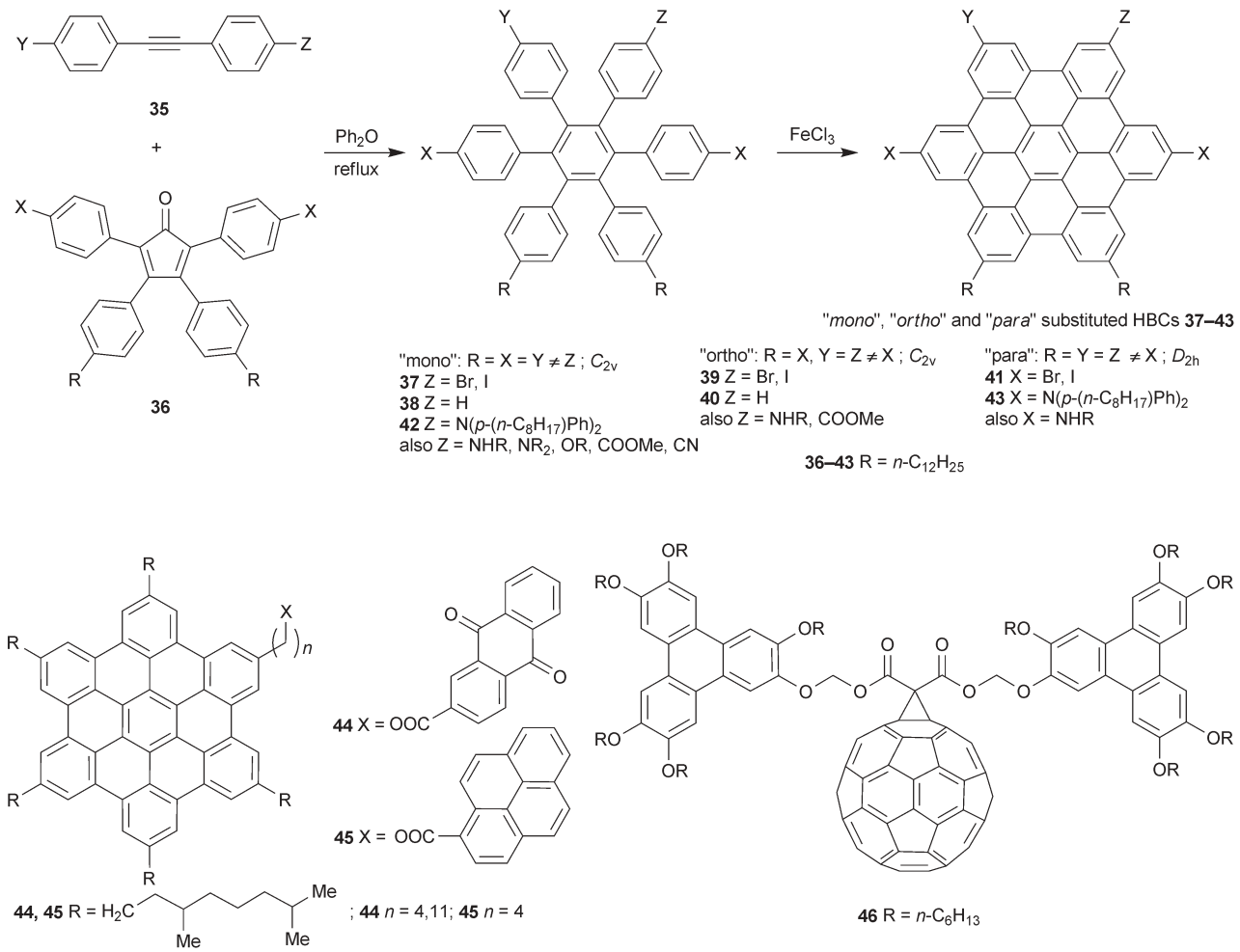

Scheme 3 Synthesis of the low-symmetry HBC derivatives (top) and examples of donor–acceptor discotic dyads (bottom).

combined effect of the substitution pattern, number of substituents and overall symmetry of the molecule on the thermotropic behavior on discotic molecules will be considered in comparison with multiply substituted HBCs.

In the series of HBC with six, five, and four alkyl substituents, the temperatures of the transitions from crystalline solids to columnar mesophases constantly increase while the isotropization temperatures remain above 400 °C (see Table 5). Thus, a reduced number of chains provides a more important effect than the lower overall symmetry of the molecule. The role of symmetry is clear, however, for the C_{2v} "*ortho*" dibromotetraalkyl HBC **39**, which melts from the crystalline solid to the columnar mesophase at significantly lower temperature than its more symmetrical "*para*" isomer **41** (Scheme 3).

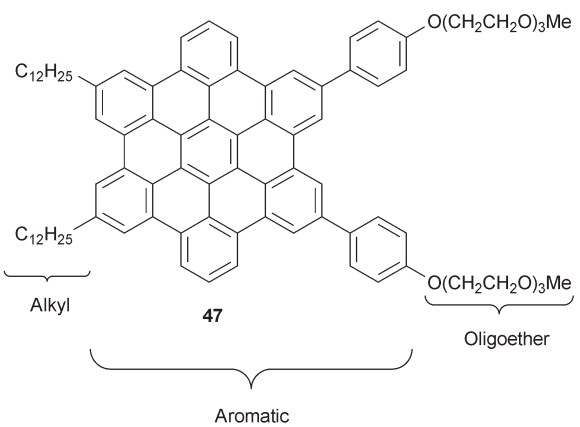

Fig. 10 Amphiphilic derivative of HBC self-assembles into giant nanotubes.[105]

In the series of PAH **39**, **48** and **49**, the overall symmetry of the molecules and the number of substituents remain the same (four alkyl chains per C_{2v}-symmetrical molecule). However, the thermotropic behavior of **49** with alkyl chains located at the zigzag sites of the periphery of the aromatic core dramatically changes compared to that of **39** and **48** (Table 5). This is undoubtedly due to the effect of a denser substitution pattern in the molecule of **49**. A similar effect of "dense packing" is observed for the D_{3h}-symmetrical molecule **50** that has a much lower first transition temperature compared to D_{6h}-symmetrical HBC **7** with less dense "packing" of the peripheral substituents.

Although discotics with a large aromatic core such as HBC and its analogs are particularly attractive since they are liquid crystalline over very large temperature ranges, low symmetry analogs of relatively small triphenylene have also received

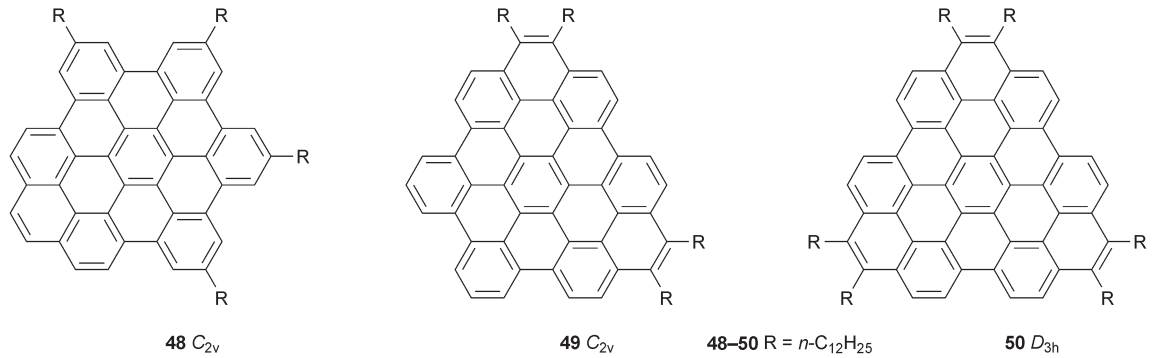

Fig. 11 Zigzag analogs of HBC.

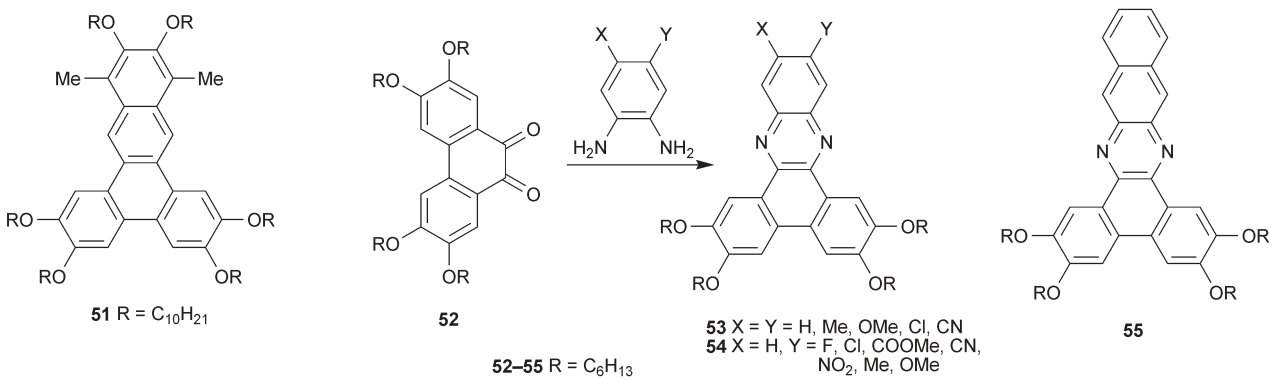

Scheme 4 Synthesis of low-symmetry analogs of triphenylene.

considerable attention. Thus, the hexaalkoxy derivative of benzo[*b*]triphenylene **51** (Scheme 4) exhibits a columnar hexagonal mesophase between 35 °C and 88 °C, *i.e.* over a broader range than the triphenylene bearing identical alkoxy substituents.[109] A versatile synthetic approach based on condensation of phenanthrene-9,10-diones **52** with commercially available *ortho*-diamines provides access to a variety of dibenzo[*a*,*c*]phenazine derivatives **53** and **54**.[110,111] Although **53** (X = Y = H) bearing four hexyloxy chains is non-mesogenic as well as its dimethyl derivative (X = Y = Me), the dicyano derivative (X = Y = CN) forms a Col_h phase with a surprisingly broad range for a relatively small core size (72–256 °C).[111] In the series of derivatives with one electron-withdrawing or electron-donating group (**54**, X = H, Y = F, Cl, COOMe, CN, NO_2, Me, OMe), a clear quantitative correlation between the tendency of these molecules to form columnar phases and substituent effect (expressed by Hammett parameters σ_m and σ_p) was obtained. Thus, molecules bearing strongly electron-withdrawing groups (NO_2, CN) form stable columnar hexagonal phases over a remarkably broad temperature range, while their analogs with electron-donating substituents directly melt from the crystalline state to the isotropic liquid. This observation can be rationalized in terms of stabilization of π–π-stacking between disc-like molecules by the addition of the electron-withdrawing groups that minimize the repulsive interactions between adjacent aromatic π-systems (see ref. 110 and references cited therein for a detailed discussion). Also the naphthalene analog **55** shows a greater tendency to π-stacking and is liquid crystalline (Col_h, 123–172 °C), probably due to the large size of the aromatic core which favors π-stacking.

Perylene diimide (PDI) dyes have found important industrial applications as dyes and pigments due to their intense optical absorption and excellent thermal, chemical and photochemical stability. Interest in discotic mesogens derived from PDI and related molecules arose from their high electron affinity which makes them very attractive as *n*-type (electron transporting) semiconductors. Since synthesis, supramolecular self-assembly and spectral properties of PDI derivatives and related compounds have been recently reviewed in detail by Würthner[112] and Langhals,[113] discussion in this review will be limited.

PDI derivatives without, or with relatively short *N*-substituents are high-melting crystalline solids. However, substitution of the imide nitrogens with sufficiently long linear alkyl substituents (*e.g.*, **56**, Fig. 12) provides liquid crystalline materials with rather complex phase behavior. Notably, a charge carrier mobility of 0.11 $cm^2 V^{-1} s^{-1}$ has been measured in the LC phase of **56**.[114] Unsaturated *N*-substituents in **57** induce formation of a lamello-columnar mesophase between 178 and 292 °C.[115] More sophisticated derivative **58** bearing *N*-trialkoxyaryl substituents forms columnar mesophases between room temperature and 373 °C.[116] Introduction of an additional CH_2 spacer between the tri(alkoxy)phenyl group and the imide nitrogen atom in **59** lowers the clearing point to 226 °C making it more readily processable from the melt.[21] A

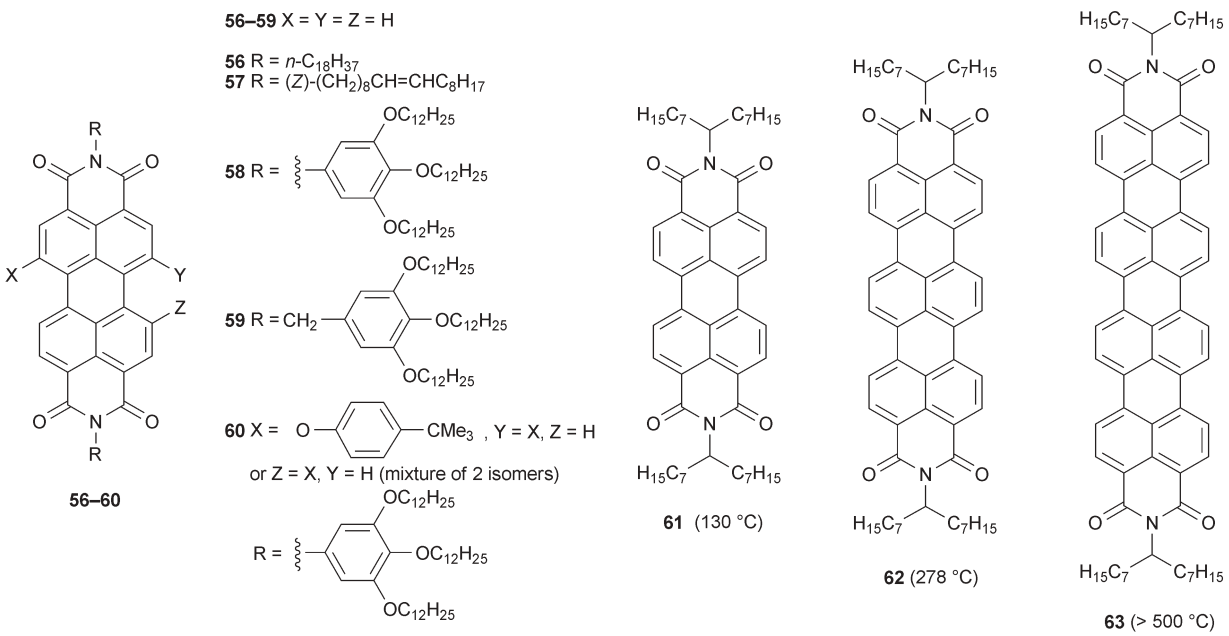

Fig. 12 Liquid crystalline rylene diimides; selected isotropization temperatures are given in brackets.

bulky substituent in the so-called bay region of the molecule also dramatically reduces the isotropization temperature (*e.g.*, 283 °C for **60**, *cf.* **58**).

The charge carrier mobility of **58** was recently studied by the steady-state space-charge limited current (SCLC) technique and was found to be highly dependent on the fabrication of samples. However, PDI derivatives were shown to be efficient electron transporting materials, and the highest value for **58** was 0.2 $cm^2\ V^{-1}\ s^{-1}$. Moreover, for its analog **59** an electron mobility of 1.3 $cm^2\ V^{-1}\ s^{-1}$, *i.e.*, higher than that of amorphous silicon, was measured under ambient conditions.[21]

Expansion of the PDI aromatic core along the long molecular axis leads to terrylene and quaterrylene diimides (TDI and QDI, respectively). Enlargement of the aromatic core is supposed to enhance the π–π-interaction which may lead to highly ordered supramolecular organization and enhanced charge carrier mobilities, as discussed above. Interesting thermotropic behavior in a series of PDI, TDI and QDI with identical branched substituents (**61**, **62** and **63**, respectively, Fig. 12) was observed.[117] With increasing core size the isotropization temperature predictably increases from 130 °C for **61** to >500 °C for **63**. However, while PDI **61** and TDI **62** directly melt from a crystalline state to the isotropic liquid and do not form LC mesophases, QDI **63** with the largest aromatic core is plastic crystalline at room temperature and forms ordered hexagonal columnar phases above 188 °C. This finding further illustrates the importance of a well-adjusted balance between the size of the core and the length of the peripheral substituents for the successful design of discotic mesogens. Probably, elongation of branched *N*-alkyl chains in the molecule of QDI would yield derivatives with accessible isotropization temperatures.

Another interesting subclass of rylene diimides are coronene derivatives such as **64** (Fig. 13), which form columnar hexagonal mesophases with rather high melting points.[118] Remarkably, a charge carrier mobility as high as 0.2 $cm^2\ V^{-1}\ s^{-1}$ was measured by the PR-TRMC method in the columnar hexagonal phase of coronene monoimide **65** at room temperature.[118] Also, structurally closely related tetraesters of perylene, coronene and ovalene tetracarboxylic acids should be mentioned here.[119] Perylene tetraesters **66** with linear substituents form columnar mesophases with reasonably low melting points[120] and have been used for the fabrication of OLEDs[121] and photovoltaic solar cells.[122] The tetraesters with 2-ethylhexyl substituents **66**, **67** and **68** (Fig. 12, 13) form columnar mesophases at room temperature and have clearing points at 260 °C, 153 °C, and >375 °C respectively.[119] These examples provide another illustration of the combined influence of various structural factors on the phase behavior of discotic mesogens. Indeed, all three molecules **66**, **67** and **68** have the same D_{2h} symmetry and the same number of identical 2-ethylhexyl substituents at the periphery of the aromatic core. As expected, the ovalene derivative **68** with the largest aromatic core has the highest clearing point. At the same time, the relatively small perylene derivative **66** has a much higher isotropization temperature compared to the coronene **67**. This is undoubtedly due to the effect of more densely positioned branched substituents in **67** that was already discussed above for HBC and its "zigzag" analogs.

2.5.3. Discotic dimers and oligomers. Molecules comprising more than one aromatic core in one molecule (referred to as "discotic oligomers") represent a very attractive class of discotic mesogens since they may, in general, demonstrate a higher degree of order compared to their "monomeric" analogs. However, "superbiphenyl" **69** (Fig. 14) prepared *via* Yamamoto homocoupling of the monobromide **37** (Scheme 3) does not form well-defined columnar mesophases. This is apparently due to intermolecular torsion that is caused by the direct linkage of the two HBC units and prevents columnar

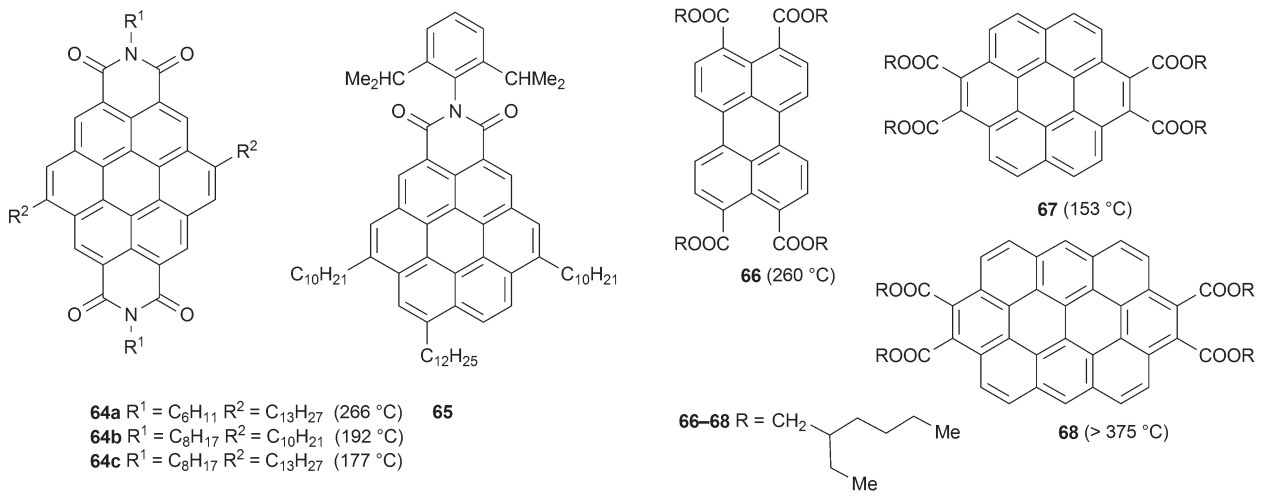

Fig. 13 Liquid crystalline derivatives of perylene, coronene and ovalene; selected isotropization temperatures are given in brackets.

self-organization. On the contrary, a "dimer" **70** with the two HBC aromatic cores connected by a sufficiently long and flexible polymethylene spacer shows only slight difference in LC behavior compared to the hexaalkyl HBC "monomer" **7** (Fig. 3).[123] In an expansion of this approach, an unprecedented star-like HBC "heptamer" **71** with six $(CH_2)_{11}$ flexible linkers between one central and six peripheral HBC units has been prepared *via* an impressive 42-fold oxidative cyclization of the corresponding precursor in a final synthetic step. At room temperature heptamer **71** forms disordered solid phases. However, with increasing temperature the HBC units become more mobile and ordered hexagonal columnar mesophases are observed.[124] In addition, in heptane or toluene solution formation of a physical gel was observed. This represents a rare case of gelation exclusively due to π–π-interaction, but without H-bonding or dipole–dipole interactions involved.

Discotic "twins" or "sandwiches" with two large aromatic cores covalently captured in a face-to-face arrangement and in close proximity to each other represent an attractive possibility for improving the inter-disc charge transport. Within this concept, cyclophane **72** (actually the cyclophane with the largest aromatic core reported to date) was prepared *via* the

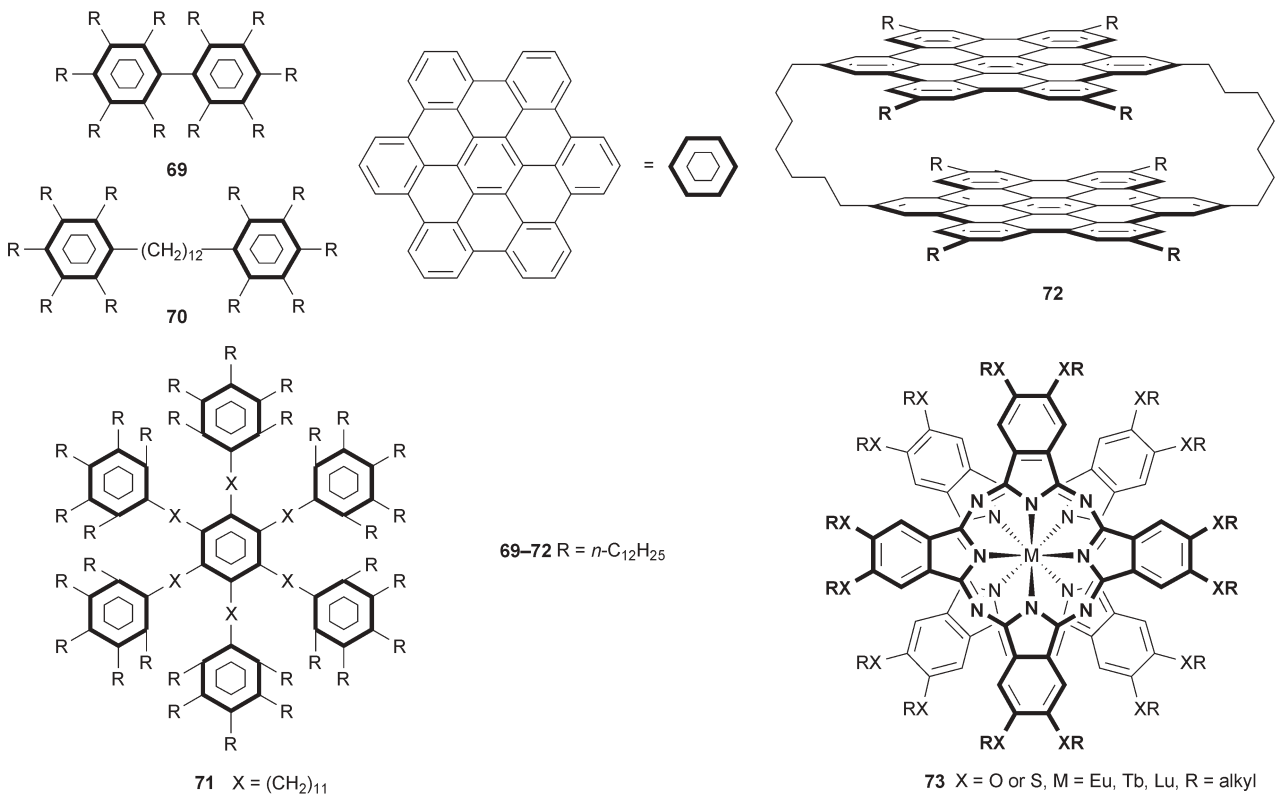

Fig. 14 Discotic twins, dimers and oligomers.

ring closing metathesis of the olefinic precursor.[125] Wide angle X-ray scattering (WAXS) of extruded fibers revealed formation of the Col_h mesophase that persists up to 400 °C. A similar design has been realized for the double-decker phthalocyanine mesogens with rare earth metal sandwiched between the two aromatic cores. The mesogens of these class form various columnar mesophases and sometimes demonstrate very complex phase behavior.[126] Notably, charge carrier mobilities as high as 0.71 $cm^2\ V^{-1}\ s^{-1}$ were reported for the lutetium "sandwich" derivative **73** (M = Lu, X = S, R = *n*-$C_{12}H_{25}$). For more detailed discussion of phthalocyanine "twins" the reader is referred to the recent review.[127]

This section, devoted to molecular concepts, has stressed the close interplay between molecular structure and properties of materials. Theory has a pivotal role to play in the rationalization of electronic properties of various molecular structures and for the design of materials with tailored electronic behavior. What is however less understood is the relationship between molecular structure and supramolecular order, which is the subject of the next section.

3. Supramolecular order and processing

3.1. Supramolecular organization of discotic molecules

Supramolecular organization of discotic molecules is closely related to molecular design.[128] At the same time, the supramolecular structure of discotics has a great influence on their performance in devices. Interactions between discotic molecules leading to their self-assembly in supramolecular structures can be governed by various non-covalent forces.[34,129] For conjugated cores, such as polycyclic aromatic hydrocarbons, π-stacking results in self-assembly into columnar stacks.[130] The microsegregation of flexible peripheral chains from the rigid aromatic core further promotes the formation of thermotropic mesophases.[131,132] However, π-stacking interactions might also result in a lateral displacement of planar aromatic cores in the columns.[133]

In blends of molecules with complementary structures, such as hexaalkoxy- and hexaphenyl-substituted triphenylenes, polytopic interactions occur from the sum of the van der Waals interactions between atoms in close contact.[134] These specific interactions in equimolar mixtures result in the alternating packing in the stacks of the differently shaped molecules accompanied by the stabilization of columnar superstructures and enhancement of electronic properties of a blend compared to the pure components.[135] When two discotic molecules with opposite electronic affinities are brought together, a similar alternating packing is observed.[115,136] Formation of donor–acceptor complexes results in the efficient charge transfer interactions between the electron-donating and the electron-accepting discs.[137]

Hydrogen bonds between a donor with relatively labile hydrogen atoms and an acceptor bearing electron lone pairs may play an important role in the self-assembly of discotic molecules. It has been shown that mesophases of disc-like molecules with an aromatic core as small as benzene are efficiently stabilized by intermolecular hydrogen bonding between amide groups.[138] Hydrogen bonding may also greatly enhance the stability of the columnar supramolecular structures formed by π-stacking.[139,140] These two forces of different nature act cooperatively leading, in some cases, to a significant lowering of the intermolecular distance within the columnar stacks (see example of HAT derivative **17** bearing six lateral *N*-alkylamide chains, Section 2).[64]

Another approach to stabilization of columnar superstructures is a coordination with metal ions. When transition metal ions such as Cu^{2+} or Co^{2+} are introduced in the porphyrin or phthalocyanine core, this results in planar molecules with tetra-coordinated metals. However, large metal ions such as lanthanides form double-decker complexes in which a metal ion is sandwiched between two phthalocyanine rings. This can lead to exceptionally small intermolecular distances. Thus, in the phthalocyanine lutetium "sandwiches" (Fig. 14) the inter-disc distance is as short as *ca.* 3.3 Å. This is reflected in mobilities up to 0.71 $cm^2\ V^{-1}\ s^{-1}$.[127]

The main thermotropic organization types which were found for these disc-like molecules can be divided into columnar,[60] discotic nematic,[141] columnar nematic[142] and lamellar (smectic-like) phases.[143] Nematic phases reveal an orientationally ordered arrangement of discs, but no long-range translational order. Fluid discotic nematic phases are commercially exploited as optical compensation films in liquid crystal displays (LCD).[144] In more viscous columnar phases the discotic molecules stack on top of each other into columns, which are in turn arranged into a two-dimensional lattice.[145] Columnar structures that are most frequently encountered in the LC phases possess a hexagonal (Col_h), a rectangular (Col_r), or an oblique (Col_{ob}) lattice.

The phase transition from the crystalline to the LC phase is accompanied by a significant increase in molecular dynamics such as the rotation of the discs around the columnar axis. In addition, both the intra- and intercolumnar organization drastically changes in comparison to the crystalline phase. The centers of gravity of molecules in columnar LC mesophases are positioned along the columnar axis and columns can slide relative to each other giving rise to the fluid character of the phase. For some systems, an intermediate mesophase is observed between the crystalline and liquid crystalline phase. In a plastic crystal phase the centers of gravity of molecules form a three-dimensional lattice whereas molecules conserve rotational freedom.[146,147] It is important to stress that the molecular fluctuations in the liquid crystalline mesophases support the self-healing of structural defects and hence enhance the charge carrier transport along the columnar stacks.[148] Due to this behavior thermotropic discotics possess essential fundamental advantages *versus* other organic semiconductors such as conjugated polymers.

The thermotropic phase behavior of discotic liquid crystals is usually studied by using differential scanning calorimetry (DSC), polarized optical microscopy (POM), wide-angle X-ray scattering (WAXS) and solid-state NMR. DSC is used to determine the temperatures of phase transitions and enthalpy changes related to each transition. The fluid character of mesophases and in many cases the characteristic textures are easily observed by POM. The supramolecular organization and the corresponding packing parameters in each phase can be studied in detail by X-ray diffraction, in particular by 2D-WAXS of macroscopically oriented samples.[60,62,89] This

technique allows one to obtain a detailed insight into the intra- and intercolumnar order. It is possible to determine not only the intercolumnar spacings but also to obtain information about the arrangement of discs within the columns, such as tilting or helical packing. Solid-state NMR is one of the most powerful tools for the study of the molecular dynamics.[149,150] This technique provides important information about the dynamics of a rigid core and flexible side chains in a molecule and allows one to derive independent conclusions about the rotation of the core or about the peripheral mobility of side chains. Moreover, because of the different electronic environments of the aromatic protons in the intracolumnar packing, the tilted arrangement of the discs in the solid phase can be determined as well. In general, it is necessary to apply all these complementary experimental methods in order to obtain a clear, comprehensive and unambiguous picture of the bulk behavior of discotic mesogens.

A generally overlooked issue is the thermooxidative degradation of discotics. This question is particularly important for their use as semiconductors and if a thermal annealing step is required during processing. Thermal stability in a given temperature range is commonly assessed by the absence of mass loss measured by thermogravimetric analysis (TGA). This convenient technique is, however, not sensitive enough to identify minor thermooxidative processes. It was shown using chemiluminescence that the onset of thermooxidative degradation of some triphenylene derivatives occurs at 130–140 °C, *i.e.* at least 100 °C below any degradation detectable by TGA.[151] Evidently, trace amounts of impurities from synthesis such as Lewis acids, oxidants and side products can further facilitate thermal degradation. Extensive purification of discotic materials and low isotropization temperatures are the best way to remedy the thermooxidative degradation during processing.

3.2 Processing

As discussed above, the ability of discotic molecules to self-assemble in columnar superstructures together with the self-healing of structural defects in liquid crystalline columnar mesophases provide great potential for their application as semiconductors for organic electronic devices. However, development of appropriate processing techniques for the fabrication of defect-free long-range oriented discotic material represents a major challenge. It has been unambiguously demonstrated that the degree of structural order plays a crucial role for the performance of semiconducting devices based on thiophene oligomers or pentacene.[5,152] The fact that the solubility and the thermal behavior of discotics can be effectively controlled "just" by the variation of flexible side chains represents a fundamental advantage for the processing. In comparison with vacuum deposition techniques, deposition of materials from solution is a remarkably more facile and potentially cheaper method for thin film fabrication.

An important issue in the processing of discotic materials is the control of macroscopic orientations of columnar superstructures on surfaces. Discotic molecules can adopt two characteristic orientations, which are required for electronic devices with different geometries. On the one hand, the planar uniaxial alignment with edge-on orientation of the molecules and columns parallel to the substrate is needed for field effect transistors (FET) (see Fig. 21, Section 4) in order to ensure the charge migration between the source and the drain. This orientation can be achieved by various alignment techniques based on the processing of material either from solution or from the isotropic state (see below). On the other hand, homeotropic alignment with a face-on orientation of the discs and the columnar axes perpendicular to the substrate is expected to be beneficial for the performance in photovoltaic cells or light-emitting diodes (LED) (see Fig. 23, 24, Section 4). Processing methods providing control over macroscopic orientation of columnar stacks relative to the surface will be discussed in more detailed below.

3.2.1. Homeotropic alignment. The face-on orientation of discotic molecules is usually a preferred mode of deposition: this process can occur during mesophase formation from the isotropic melt or *via* the deposition of a dilute solution onto the surface. By changing the chemical nature of the aromatic core and/or of the side chains it is possible to modify the surface affinity of the molecules.[153] Monolayers of discotic molecules "lying flat" on the substrate can be obtained by deposition of dilute solution onto MoS_2 or highly oriented pyrolytic graphite, as reported for discotic triphenylenes,[154,155] hexaazatriphenylene **17**[156] (Fig. 7) and HBCs.[102,157] In these cases, the main driving force for the face-on organization is the interaction between the disc and the surface. The supramolecular arrangement of self-assembled triphenylenes on a gold surface was controlled by the number and position of the thiol anchor groups attached to the disc-like core.[158]

The face-on orientation of discotic molecules obtained by slow cooling of the material from the isotropic phase can initiate the formation of homeotropic alignment on a macroscopic scale. The molecules arranged on the surface act as nucleation sites at which new discs self-assemble in columns. Typically, this process occurs during annealing at the isotropic liquid to mesophase transition where the mesophase viscosity is low.

Homeotropic alignment between two solid substrates has been reported for many different discotic molecules and is independent of the core size and film thickness.[48] It occurs for columnar mesophases as well as for less viscous discotic nematic mesophases, as recently demonstrated with a porphyrin derivative.[159] However, there are essential differences between the alignment on one or between two solid substrates. Only very limited examples of successful homeotropic alignment on *one* solid substrate have been described,[19,160–162] while the self-alignment of the discs was strongly dependent on the film thickness.

In the specific case of phthalocyanine **18e** (Fig. 8) the air interface has proven to govern the alignment for film thickness ranging from 50 nm to several μm and never gave a homeotropic alignment.[7] One way to circumvent the absence of the spontaneous homeotropic alignment when an air interface has to be present (*e.g.*, when subsequent deposition of other layers on the top of homeotropically aligned discotic material is foreseen) consists in the use of a sacrificial polymer layer (Fig. 15).[163] After inducing the desired homeotropic alignment the sacrificial layer is simply washed away with a

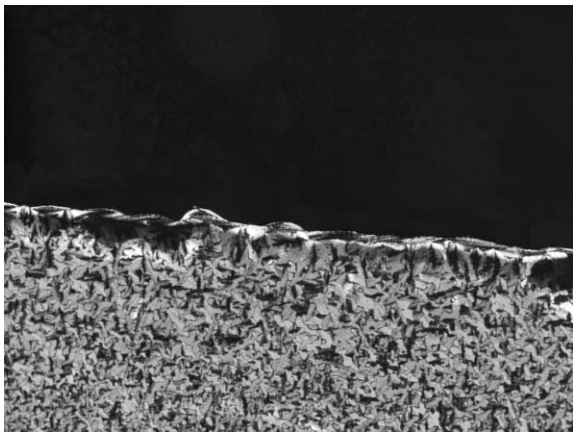

Fig. 15 Thin film of phthalocyanine **18e** after heating above the isotropization temperature and subsequent cooling to the ambient temperature, POM image. The upper part of the image appears black due to homeotropic alignment: this part of the sample was covered with a sacrificial layer (polyvinylphenol). The lower part of the image reveals mosaic texture typical for the columnar mesophase: this part of the sample has an interface with air.

suitable solvent that must obviously leave intact the homeotropically aligned discotic layer.

The "molecular ingredients" leading to the spontaneous face-on orientation of discotic molecules between two solid substrates have not been yet identified. In many cases, the aromatic cores were substituted by side chains bearing heteroatoms, which might enhance the affinity of the molecules to the surfaces and thus the tendency to form homeotropic alignment (see HBC **74**).[86,164–168] However, the formation of homeotropic alignment by an all-hydrocarbon HBC **75**[71] (Fig. 16) and even by larger PAHs[169] indicates a more complex mechanism. This is further assessed by the homeotropic alignment of phthalocyanine **18e** (Fig. 8) that occurs between a variety of substrates including gold, glass, ITO (indium–tin oxide), PEDOT-PSS (poly(3,4-ethylenedioxythiophene)-poly(styrenesulfonate)) and polyisobutylene

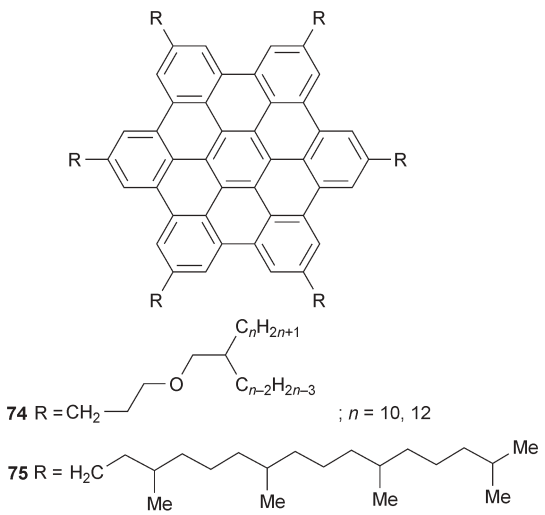

Fig. 16 Some HBC derivatives that spontaneously form homeotropic alignment.

rubber.[7] It has recently been shown that homeotropic alignment between two solid surfaces of various natures can be induced by the introduction of appropriate partially fluorinated chains at the periphery of triphenylene molecules (see also Fig. 3 and Table 4).[82] These observations seem to indicate that homeotropic alignment between two solid substrates is achieved regardless of the chemical nature of the surfaces. However, such a conclusion is incorrect in the light of the recent works of Kato[170] and Nolte[171] who could demonstrate that homeotropic alignment is indeed induced by specific molecule–surface interactions such as hydrogen bonding or metal coordination. In addition, homeotropic alignment also occurs for miscible blends of dissimilar discotic molecules[115] and for donor–acceptor discotic dyads.[102,103]

It is rationalized from these, sometimes contradictory, results that a subtle balance between the enthalpy (molecule–substrate interactions) and the entropy (conformations of side chains) controls the occurrence of homeotropic alignment. These views are supported by the fact that the temperature of thermal annealing required to induce homeotropic alignment is sample-specific and varies considerably. An annealing temperature as high as 1200 °C was used in a somewhat different case of the mesophase-pitch-based carbon layers. During carbonization process, the disc-like graphite fragments orient preferentially edge-on on some metals and all oxides, with the exception of mica. Face-on anchoring is observed on carbon graphene planes, mica and metals (Pt, Ni and Ag).[172] Besides thermodynamics, the kinetics of growth also influences the alignment of liquid crystalline discotics. Very recently, it has been shown that the competition between planar and homeotropic alignment can be controlled by the kinetics of annealing.[162] Finally, homeotropic or linear alignment can be created by an external stimulus such as polarized infrared irradiation of liquid crystalline or plastic crystalline columnar mesophases.[173]

Homeotropically aligned samples typically do not show birefringence in the POM between cross-polarizers (Fig. 17a), since the optical axis in this case coincidences with the columnar axes. In order to distinguish between the homeotropically aligned columnar and the isotropic phase, additional experiments are necessary. X-Ray scattering is one method which confirms precisely the alignment (Fig. 17b). FTIR spectroscopy, as an alternative technique, points out also the orientation of the aromatic core on the substrate. Typically, the C–C aromatic stretching vibration and the C–H out-of-plane vibration can be directly correlated with the face-on arrangement of the disc-like molecules in the homeotropically aligned LC phase.[174,175]

It has been shown that improved homeotropic order within an indium–tin oxide (ITO) cell improves the photoconductivity by a factor of five compared to poorly oriented parts of the sample.[71] Another efficient way to determine the relationship between the homeotropic alignment and electronic properties of an organic semiconductor is time-of-flight experiments.[176] The determined charge carrier mobility is strongly dependent on the thermotropic behavior as well as on the alignment of the material.[177] Pronounced intracolumnar order, such as helical arrangement,[39] and self-healing in the LC phase lead to higher mobilities along columnar structures, whereas columnar

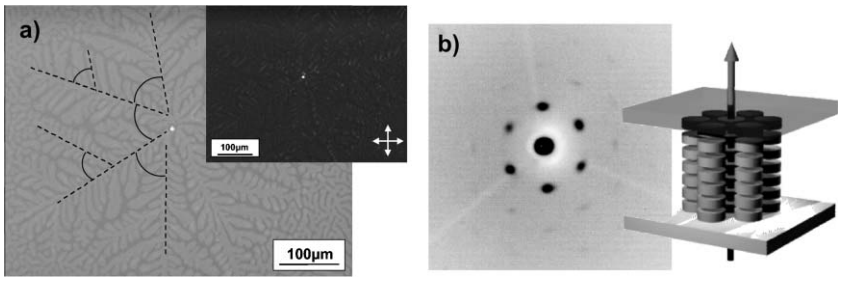

Fig. 17 Example of a homeotropically aligned HBC **72b** (Fig. 16): (a) the dendritic texture obtained by cooling the sample from the isotropic phase between two surfaces appeared black in the POM, which is characteristic for homeotropic alignment; (b) 2D-WAXS confirmed the orientation revealing a typical hexagonal pattern that suggests a uniform organization of the columns over large areas (inset: schematic illustration of the columnar alignment towards the incident X-ray beam).[161]

disorder limits the one-dimensional charge transport. The created charge carriers migrate through the well-aligned sample in a non-dispersive manner, while disperse transport was observed for non-oriented samples and for materials in the crystalline state due to charge-trapping at macroscopic grain boundaries.[148]

3.2.2. Planar alignment. It has been shown in the previous section that no homeotropic alignment could be obtained with an air interface. Instead a planar alignment with a random distribution of the column directors in the plane parallel to the air interface has been observed. Such alignment is of little practical interest if discotic mesogens are designed for charge transport applications. A uniaxial planar alignment with the columns parallel to the substrate but with long columnar axes pointing in the same direction is obviously preferable for electronic devices such as field effect transistors (FET). Uniaxial alignment can be obtained in Langmuir–Blodgett (LB) films.[178] During the dipping of the substrate into and out of water the discs, which self-organize at the air–water interface, are deposited. Typically, a macroscopic planar alignment of the columns with their long axis parallel to the dipping direction is observed. Discotic molecules orient edge-on at the air–water interface if they bear hydrophilic groups on one side chain.[179–181] In order to improve the organization of amphiphilic molecules in LB films, functionalization of the substrate by poly(ethylene imine) which acts as an anchor point for the first deposition layer can be used.[182,183] In some cases, symmetrical discotic mesogens without any amphiphilic character arrange edge-on and generate stable columnar assemblies at the air–water interface.[184,185] In other cases, the introduction of hydrogen bonds leads to a face-on orientation with the discs "lying flat" on the water surface and the hydrocarbon chains extending away from the water interface.[186,187] This obviously precludes the formation of the desired uniaxial alignment.

Planar alignment has also been achieved in a metal–SAM–metal junction (SAM: self-assembled monolayer) with an HBC derivative bearing a dithiolane functionality. This allowed one to observe the tunneling of electrons across columns and to reach the conclusion that HBC units are transparent to electrons as compared to aliphatic chains.[188]

Another way to achieve a uniaxial alignment of columns is the use of an alignment layer to benefit from epitaxial growth. A breakthrough in the epitaxial growth of various materials on friction pre-oriented poly(tetrafluoroethylene) (PTFE) surface layers was achieved by Wittmann and Smith.[189] There are two examples of PTFE-aligned discotic liquid crystals. Thus, a triphenylene derivative was spin-coated onto the PTFE orientation layer and after evaporation of the solvent, a uniaxial in-plane alignment of columns along the orientation direction was determined from the high optical anisotropy observed in polarized optical microscopy and absorption.[12] Annealing of the films at higher temperatures (in the Col_h mesophase) further increased the degree of orientation.

An identical alignment was observed for larger PAHs, such as hexa-substituted HBCs **8** and **19f** (Fig. 3 and Fig. 8) that were deposited from solution onto the PTFE film.[13,14] The structure evaluation by grazing-incidence X-ray diffraction and the high optical anisotropy in polarized absorption indicated well-aligned HBC films with a parallel orientation of the columnar stacks on the underlying PTFE chains.[13,190] The epitaxial organization of the two-dimensional lattice describing the columnar arrangement fitted with a certain number of the PTFE chains as Wittmann had predicted for a successful alignment.

The zone processing methods are based on a change of the processing conditions such as temperature, deformation rate or solvent concentration within a defined zone resulting in a parameter gradient which is the driving force for the directed growth.[191] This enables a quite facile way to produce uniaxially aligned thin films without the use of an alignment layer. The principle of zone processing is schematically shown in Fig. 18. For zone casting, a solution is spread by means of a nozzle onto a moving support, creating a concentration gradient within a meniscus formed between the nozzle and the support. At the critical concentration the material nucleates from the solution onto the moving substrate to form a uniaxially aligned thin layer.

This alignment technique has been successfully applied for PAHs with extended aromatic cores that demonstrate pronounced self-aggregation in solution.[192] Moreover, it was demonstrated that such pre-aggregation is beneficial for the formation of highly ordered uniaxially aligned films. The structural evaluation of these thin films revealed columnar structures uniaxially oriented in the deposition direction with exceptionally high column length[9,10,193] and a "quasi single-crystalline" supramolecular structure with edge-on arranged

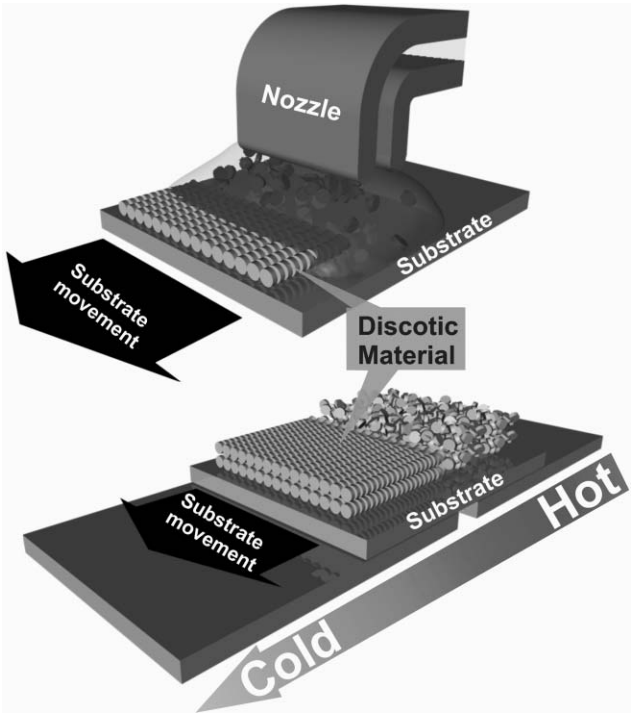

Fig. 18 Schematic illustration of zone casting (top)and zone crystallization (bottom) of discotic molecules.

molecules (Fig 19b,c).[194,195] Due to rotation of the discs from a herringbone arrangement in the crystalline state to the cofacial, non-tilted packing in the LC phase the optical anisotropy could be changed upon heating from zero to a highly anisotropic film.[196]

The uniaxial alignment from the melt along a temperature gradient has been exploited by Liu and Bard.[197] Their zone-melting technique was based on an electrically heated wire which generated a narrow molten zone on the organic layer sandwiched between two glass slides. When the molten zone was slowly moved across the sample, a single-crystal film was produced after a single pass. An additional effect was the significant improvement of the purity of the materials due to the zone-refinement.

As described above, it was essential for the melt processing of discotics consisting of larger aromatic cores to decrease their isotropization temperatures by substitution with bulky, branched side chains (see Section 2). These sterically demanding substituents reduced self-aggregation and led to the formation of macroscopically ordered domains as observed for the HBC derivative **19e** (Fig. 8). The columns were radially oriented in the spherulites indicating pronounced tendency for long-range self-organization (Fig. 19a).[77]

This pronounced directed growth of **19e** opened up the opportunity to align the material by zone-crystallization (Fig. 18). Upon moving a sample along the temperature gradient with a constant speed, the material crystallized in the oriented film. 2D-WAXS revealed a columnar growth along the temperature gradient with edge-on arranged discs, and POM displayed high optical anisotropy characteristic for a macroscopically oriented layer.

3.2.3 Tubes and fibers. Wendorff and coworkers recently used porous alumina templates to produce aligned liquid crystalline triphenylene nanowires.[198] When the pores with a diameter of a few hundred nanometres were filled with the molten triphenylene derivative, only the pore walls were wetted by the material. It has been observed that various parameters, such as pore geometry, interfacial phenomena and the thermal history, influence the order of the discs within the pores. A further development of this tempting method was the preparation of nanotubes consisting of a polymer layer outside the tube and a discotic triphenylene layer inside. Under controlled annealing in the mesophase, the discs rearrange to produce a columnar alignment along the axes of the tubes.[199] Recently, HBC **19e** was successfully templated in nanoscopic pores as well as in macroscopic glass capillaries by melt processing. In both cases, the columnar structures were long-range aligned along the template axis. This behavior was explained by the pronounced directional self-assembly of the **19e** molecules, while the influence of template curvature was negligible.[200] An alternative to produce stable graphite nanotubes was presented for discotic HBC derivatives.[201] The filling of membrane pores with a solution of material resulted in a wetting of the walls. After carbonization at high temperatures and removal of the inorganic template, carbon nanotubes consisting of ordered graphene sheets oriented perpendicular to the tube axis were obtained.

Fibers are structurally related to nanotubes by their high aspect ratio. Triphenylene and phthalocyanine derivatives self-assemble out of solution into fibers with well-defined internal structure and controlled external geometry.[202,203] Floating phthalocyanine fibers in dodecane solution have been shown to adhere in a planar way to an ITO substrate in the absence of

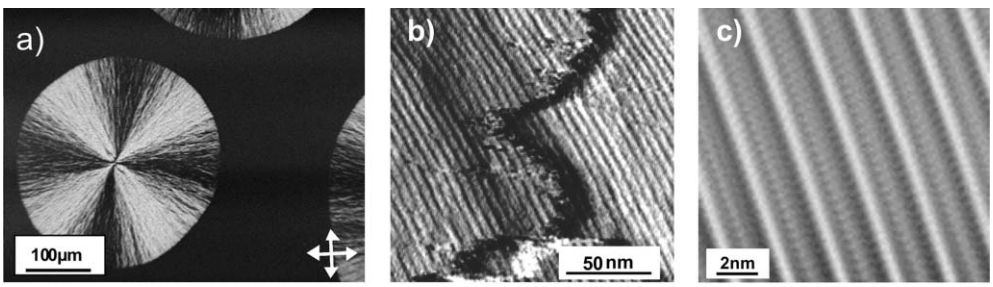

Fig. 19 (a) Formation of spherulitic domains by cooling **19e** from the isotropic phase, (b) AFM image of zone-cast uniaxially aligned HBC derivative **7** revealing also underlying columnar structures, (c) inverted FFT image of zone-cast **7** from the high-resolution electron microscopy.

an electric field. When the electric field is turned on, the fibers "stand up" with their long axes oriented in the direction parallel of the electric field.[203]

The major conclusion from this section is that disc-like molecules can be processed in highly ordered thin films with tailored alignment. This is an important prerequisite for the study of electronic properties of discotic mesogens and their use in the devices.

4. Charge transport and optoelectronic devices

4.1. Charge transport in bulk and thick films

A comprehensive study on charge transport in columnar mesophases has been carried by Warman and collaborators using the pulse-radiolysis time-resolved microwave conductivity (PR-TRMC) technique which reveals local mobilities of charge carriers that migrate between only a few molecules.[204,205]

Mobilities in the bulk measured by the time-of-flight (TOF)[147,206–209] or field-effect transistor (FET) techniques are usually several orders of magnitude lower due to a higher degree of disorder and possible trapping sites at grain boundaries. The latter values are strongly dependent also on the long-range order of the columnar structures which can be controlled by different processing techniques. The charge carrier mobilities obtained by the PR-TRMC technique can be considered as the maximum possible values reflecting the properties at the molecular level while TOF and FET measurements reflect the supramolecular organization. Furthermore, it was proven that the peripheral substitution of the aromatic cores with long aliphatic hydrocarbon chains provides an insulation of the conducting core and columnar stacks of disc-like molecules can thus be considered as "nanowires". It has been shown that the life-time of charge carriers within the columnar stacks of HBCs and phthalocyanines increases with increasing length of alkyl side chains and this confirms the insulating action of the substituents.[210]

A disadvantage of the PR-TRMC technique is its insensitivity to the sign of charge carriers, that is, it does not allow one to distinguish between mobility of holes and electrons. In contrast, TOF gives an opportunity to study the charge transport of electrons and holes and in addition, reveals the effect of alignment on the charge carrier mobility, as discussed above. In most cases only the transport of holes was observed with maximum mobilities of *ca.* 0.1 $cm^2\ V^{-1}\ s^{-1}$ for highly ordered phases of triphenylenes[39,211] and phthalocyanines.[212] The absence of a TOF signal for electrons was assigned to the oxygen trapping of the negative charge carriers. Recently, the high TOF electron mobilities of 0.01 $cm^2\ V^{-1}\ s^{-1}$ for hexabutyloxytriphenylene in the hexagonal plastic phase[213,214] and even 0.08 $cm^2\ V^{-1}\ s^{-1}$ for hexahexylthiotriphenylene in the highly ordered helical phase have been reported.[215] In the latter case, the electron transport was strongly dependent on the purity of samples. Insufficiently pure samples revealed only a disperse TOF signal suggesting specific trapping of the negative charges.

The best way to differentiate the electronic mobility from the mobility of ionic impurities is to dilute a discotic liquid crystalline mesophase with an inert solvent such as a linear alkane. Alkanes do not contribute to the electronic charge transport, thus, the mobility in diluted samples decreases if the electronic transport mechanism predominates. The opposite is observed for ionic transport due to decreased viscosity.[214] However, such experiments that are tedious but highly necessary for reliable structure–property assessment are rather scarce.

Other TOF measurements carried out in the group of Iino and Hanna on octaalkyl phthalocyanine **76** (Fig. 20) have revealed ambipolar charge transport with hole and electron mobilities of 0.2 and 0.3 $cm^2\ V^{-1}\ s^{-1}$, respectively.[23,212] What is remarkable is that experiments repeated in the absence or in the presence of oxygen gave comparable electron mobilities. As mentioned above, PDI derivative **59** (Fig. 12) exhibits even higher electron mobility (1.3 $cm^2\ V^{-1}\ s^{-1}$), probed by space charge limited current (SCLC) under ambient conditions.[21]

These values of charge carrier mobility obtained by different methods and with various molecular structures prove that the electron transport is fairly independent of the electron affinity of the molecules and that the perturbing impact of oxygen on the electron transport might be more complex than initially believed on the sole basis of redox potentials.[216] It seems that electron deficient and low band gap discotics are also excellent organic semiconductors for both positive and negative charge transport. It makes this kind of materials even more promising for device applications.

Dependence of the charge carrier mobility values on temperature and electric field also provides important information on charge transport mechanisms.[176,217–220] Based on the theoretical concepts introduced in Section 2, it is assumed that charge transport mechanism, *i.e.* hopping[42] or band-like transport[63,220] would be sample-specific since the magnitudes of the nearest-neighbor electron transfer integral and of dynamic disorder energies change considerably with a variation of molecular structure and supramolecular order.[19,42,56] If one considers in addition the dramatic influence that minor amounts of impurities might have on charge transport, it is not surprising that various temperature and electric field dependences are observed.[54,214] Furthermore, Bard and co-workers have demonstrated in photoconductivity experiments the influence of pressure on one-dimensional charge transport in columnar stacks of porphyrin derivatives. A sharp increase in photocurrent that could indicate a transition form hopping to

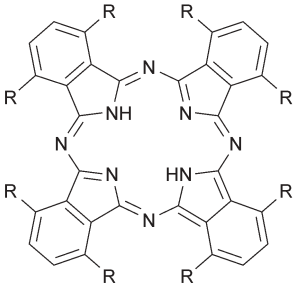

76 R = *n*-C_8H_{17}

Fig. 20 Phthalocyanine **76** demonstrates high ambipolar TOF charge carrier mobility.

delocalized conduction was observed upon pressure increase.[221]

4.2. Charge transport in thin films

It appears clear from the above that aromatic discotic molecules possess the necessary electronic properties, in particular high charge carrier mobilities, for their prospective applications in electronic devices. On the other hand, we have shown that the properties of discotic materials depend strongly upon their supramolecular structure and the macroscopic orientation of columnar superstructures on the surfaces. Although both supramolecular organization and macroscopic alignment can, in general, be efficiently controlled by suitable processing methods, fabrication of realistic electronic devices remains a major challenge. In this last section we will briefly review the known examples of successfully operating devices based on discotic semiconductors.

4.2.1. Field effect transistors (FETs). An important requirement for the implementation of discotics in FETs is the uniaxial alignment of the columns on the surface of the gate electrode to create a bridge between the source and the drain (Fig. 21). By applying an adequate gate voltage, it is possible to accumulate charges at the first monolayers resulting in source–drain current flow.

Solution processing onto pre-oriented PTFE layers or zone-casting effectively orients discotic molecules into highly ordered thin films. PTFE-aligned films of hexaalkyl-HBC derivatives showed promising device performance with mobilities up to 10^{-3} cm^2 V^{-1} s^{-1} along the alignment direction. The corresponding values for non-aligned films of the same material were two orders of magnitude lower, confirming the importance of the long-range order for the performance of devices.[14] The on/off ratio was more than 10^4 with a turn-on voltage of *ca.* −5 V to −10 V. A significant device improvement has been obtained for thin surface layers of HBC derivative **7** (Fig. 3) prepared by the zone-casting technique.[10] An on/off ratio of 10^4 and a higher mobility (5×10^{-3} cm^2 V^{-1} s^{-1}) were obtained. The superior device performance was attributed to the "quasi single-crystallinity" of **7** that was induced by the zone-casting.[195]

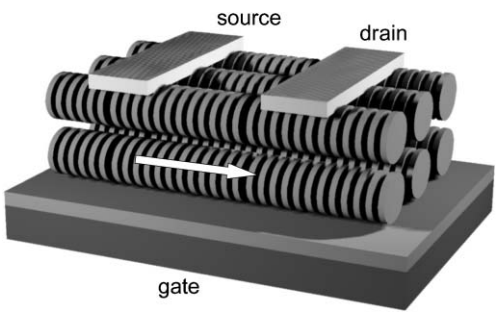

Fig. 21 Schematic illustration of a top-contact FET based on edge-on arranged discotic molecules and uniaxially aligned columns connecting the source–drain contacts. The arrow indicate the direction of the charge carrier transport within the first monolayers.

However, in all cases the charge carrier mobilities in FETs were *ca.* two or three orders of magnitude lower than the charge carrier mobility obtained by PR-TRMC.[72] This significant difference was related to the presence of local intracolumnar packing defects which constitute localized barriers for charge carrier motion along the columns. The work of Wasielewski and coworkers brings additional information about this issue. FETs have been fabricated with vapor or solution deposited films of PDI **77** (Fig. 22).[22] Electron mobilities ranging from 0.10 to 0.64 cm^2 V^{-1} s^{-1} were measured for vapor deposited films whereas values an order of magnitude inferior were obtained by solution processing. These results suggest that the mobility discrepancy between vapor and solution processed films is not due to the oxygen trapping of the charge carriers, since these devices are air-stable, but should be related to purity, film morphology and/or poor contact with source and drain electrodes.

Armstrong and co-workers have fabricated Langmuir–Blodgett films of phthalocyanine discotics on interdigitated electrodes and FET substrates. Despite the fact that the disc-like molecules self-organize into columnar aggregates with coherence lengths as large as 300 nm, mobilities remain rather low, *i.e.*, between 10^{-4} and 10^{-6} cm^2 V^{-1} s^{-1}.[222] However, mobilities of *ca.* 10^{-2} cm^2 V^{-1} s^{-1} have also been reported for the same phthalocyanine discotics.[223] This illustrates that performance of materials is closely related to the fabrication of devices.

4.2.2. Photovoltaic solar cells. It has been demonstrated with solution processed polymers and vapor deposited pigments that heterojunction photovoltaic cells consisting of blends of donor and acceptor organic materials show the best performances. During absorption of light an exciton is created and diffuses to the donor–acceptor layer boundary where it is separated into a hole and electron. High charge carrier mobilities of material and long exciton diffusion length prevent the trapping of the excitons and ensure efficient charge separation.[224] In this context, discotics that combine large exciton diffusion length[24] and high charge carrier mobility[20–23] appear to be ideal active materials for photovoltaic cells (Fig. 23).

However, several difficulties arise at this point. First of all, the miscibility of discotics that could even form alternating stacks of donor and acceptor molecules will be detrimental for the charge transport.[115,137] Then, charge transport may further be hindered by the lack of homeotropic alignment. Such alignment that may be induced by the electrode interface for the neat components may be, at the same time, perturbed by a

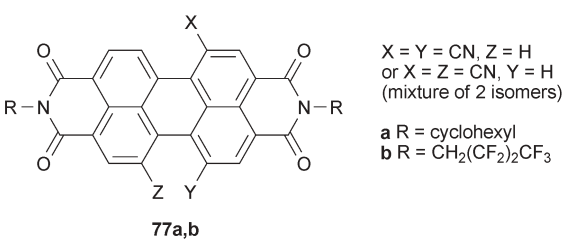

77a,b

Fig. 22 PDI derivatives used for the fabrication of FETs.

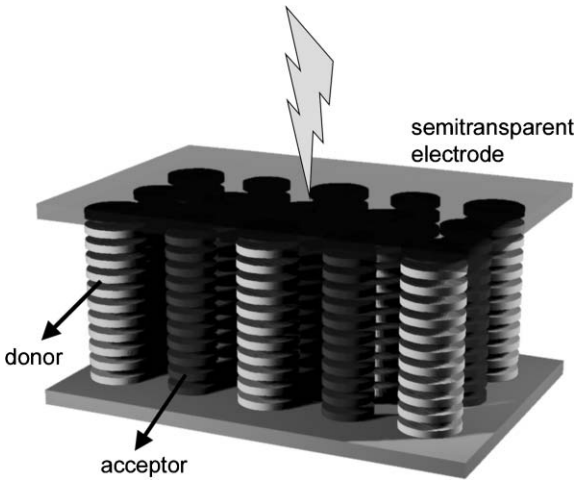

Fig. 23 Schematic arrangement of donor and acceptor discotic molecules to give a microseparation of the columnar structures in the photovoltaic cell.

much larger donor–acceptor interface. The only proven example of homeotropic alignment of a two-component system has been obtained for miscible blends.[115] Finally, the morphology is anticipated to play a crucial role in charge and exciton transport. The extent of the phase separation should not exceed the exciton diffusion length in order to provide its efficient separation into opposite electronic charges.[225]

All photovoltaic cells based on discotics consist of a two-layer system with derivatives of perylene diimide (PDI) as an acceptor compound and electron conducting material. However, these devices revealed relatively poor external quantum efficiencies (0.5% for phthalocyanines[226] and 3.0% for triphenylene derivatives[227] as donor components). The use of HBC derivative **8** (Fig. 3) resulted in a significant improvement of the device performance, also due to enhanced control of morphology.[228] Spin-coating produced a vertical gradient of PDI due to its lower solubility of both compounds separated by a rough interface. A photovoltaic cell with external quantum efficiency as high as 34% at a wavelength of *ca.* 490 nm was obtained. The hexaalkyl HBC **19f** (Fig. 8) resulted in a solar cell with an efficiency one order of magnitude lower, but still significantly higher than the first two examples.[229]

Hexadodecyl HBC **7** (Fig. 3) and an *N*,*N*′-dialkyl PDI derivative have been blended in thin films that were annealed while in conformal contact with a flat elastomeric stamp. The latter restricts the top surface of the thin film during annealing, leading to low surface roughness. An external quantum efficiency of 29.5% was measured at 460 nm.[230]

These few attempts to fabricate solar cells with discotic semiconductors has obviously not revealed all their potential since homeotropic alignment of mutually non-miscible discotics with a 10–100 nm phase separation scale has not been achieved yet. The 34% external quantum efficiency must thus not be seen as an upper limit but instead as a milestone towards highly efficient discotic-based solar cells.

4.2.3. Light-emitting diodes (LED). In an OLED the active organic components are sandwiched between two electrodes, one of which is transparent. Fig. 24 illustrates an anticipated optimal columnar arrangement in a double-layer OLED configuration consisting of an electron-rich donor and electron-poor acceptor. After injection of the electrons into the LUMO of the acceptor and of the holes into the HOMO of the donor, the charge carriers drift through the sample under the influence of an external electric field. At the layer boundary the electron and hole form an exciton that recombines to produce luminescence. For efficient devices, it is important that the energy levels are matched to minimize barriers for carrier injection and at the luminescent region.[231,232]

Double-layer OLEDs consisting of the electron-rich triphenylene (hole transporting material) and the electron-deficient perylene (electron transporting material) is an interesting alternative to other systems, since saturated red light emission from OLEDs is less common than green or blue emission. Most organic red light emitting devices are based on rare earth complexes and amorphous conjugated polymers, which exhibit stability problems and are difficult to purify. The groups of Bock and Destruel, pioneers in the development of OLEDs based on columnar discotics, observed a stable performance with a red electroluminescence for a double-layer OLEDs with a sandwiched configuration.[233] Although the supramolecular order in both layers was not controlled, other results for similar configurations suggested the importance of structure control for device performance leading to higher quantum efficiencies.[234] Another obvious candidate for red light emitting OLEDs is the star-shaped pyrene derivative **24** (Fig. 9) that exhibits a record quantum yield of fluorescence in the solid state.[25]

In summary, a few devices fabricated with discotic semiconductors have shown promising performance and call for further improvements and optimization. In particular, it should be stressed that discotics **76** and **77** are amongst the best air stable ambipolar organic semiconductors known to date.

5. Conclusions and perspectives

The overall objectives of the research conducted on discotic semiconductors are to achieve the control of: (i)

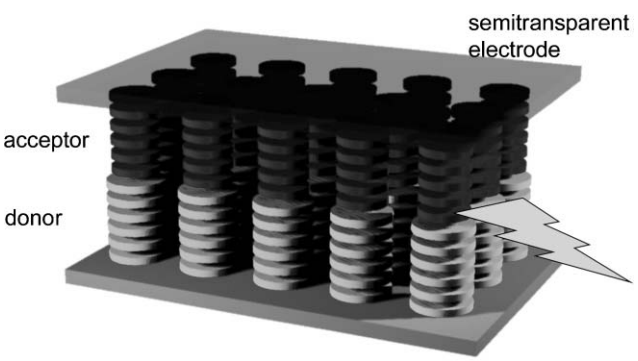

Fig. 24 Schematic arrangement of donor and acceptor discotic molecules forming a double layer in the LED.

function through molecular structure and supramolecular order; (ii) order from nm to mm scales; (iii) alignment to reach performance in devices and finally (iv) to link charge transport to dynamics and supramolecular order. Although the field of discotics as semiconductors is still in its infancy, impressive achievements have been obtained.

Original disc-like molecules of unprecedented size and structure have been synthesized. Their thermotropic behavior, solid state packing, alignment and processing have been tailored with the structural modifications of their side chains. The availability of pure discotic mesogens in sufficient amounts and with tailored mesophases has prompted their studies as semiconductors. It has become evident that the electronic delocalization in the x,y plane of the molecules and in the z direction of the column axes presents unusual aspects: (i) low band gap and low reorganization energies associated with the chemical stability in ambient conditions, (ii) high charge carrier mobility for electrons even in the presence of water and oxygen, (iii) high sensitivity of charge transport to structural defects and dynamics due to its quasi one-dimensional character, (iv) bandwidth comparable to that of graphite, (v) high quantum yield of fluorescence, and (vi) large exciton diffusion length, to mention only the most prominent features.

It is stressed that the two-dimensional delocalization of electrons which is characteristic for disc-like molecules leads to molecular electronic features that are not observed in linear oligomers and polymers. In addition, molecular electronic properties are amplified at the supramolecular level due to the extended interactions between π-systems. Therefore, discotics are a truly new generation of organic semiconductors, even if they have seldom been exploited in devices until now. Considerable work on device fabrication and optimization is obviously needed to uncover the full potential of discotic semiconductors.

Numerous perspectives of new and exciting research exist, notably the control of supramolecular order, the miscibility and the morphology of discotic blends, the understanding of solution self-assembly and its translation into solid state packing, the use of helical columnar structures for generation of large non-linear optical responses, the combination of charge transport with magnetic properties, and the incorporation of columnar structures in membranes.

Acknowledgements

The work presented in this review is the result of several research networks: EU-funded NAIMO (No NMP4-CT-2004-500355) and DISCEL (No G5RD-CT-2000-00321), SOLPLAST supported by the Walloon Region, ARC 00/05-257 supported by Communauté Française de Belgique and SOLTEX funded by the Belgian Federal Science Policy Office. We thank Klaus Müllen, John Warman, Jérôme Cornil, Roberto Lazzaroni and other colleagues and coworkers for their contributions and fruitful discussions.

References

1 *Electronic Materials: the Oligomer Approach*, ed. G. Wegner and K. Müllen, Wiley-VCH, Weinheim, 1998.
2 *Semiconducting Polymers: Chemistry, Physics and Engineering*, ed. G. Hadziioannou and P. F. van Hutten, Wiley-VCH, Weinheim, 2000.
3 F. J. M. Hoeben, P. Jonkheijm, E. W. Meijer and A. Schenning, *Chem. Rev.*, 2005, **105**, 1491–1546.
4 J. Elemans, A. E. Rowan and R. J. M. Nolte, *J. Mater. Chem.*, 2003, **13**, 2661–2670.
5 C. D. Simpson, J. S. Wu, M. D. Watson and K. Müllen, *J. Mater. Chem.*, 2004, **14**, 494–504.
6 J. Tant, Y. H. Geerts, M. Lehmann, V. de Cupere, G. Zucchi, B. W. Laursen, T. Bjornholm, V. Lemaur, V. Marcq, A. Burquel, E. Hennebicq, F. Gardebien, P. Viville, D. Beljonne, R. Lazzaroni and J. Cornil, *J. Phys. Chem. B*, 2005, **109**, 20315–20323, (*erratum: J. Phys. Chem. B*, 2006, **110**, 449).
7 V. de Cupere, J. Tant, P. Viville, R. Lazzaroni, W. Osikowicz, W. R. Salaneck and Y. H. Geerts, *Langmuir*, 2006, **22**, 7798–7806.
8 A. J. J. M. van Breemen, P. T. Herwig, C. H. T. Chlon, J. Sweelssen, H. F. M. Schoo, S. Setayesh, W. M. Hardeman, C. A. Martin, D. M. de Leeuw, J. J. P. Valeton, C. W. M. Bastiaansen, D. J. Broer, A. R. Popa-Merticaru and S. C. J. Meskers, *J. Am. Chem. Soc.*, 2006, **128**, 2336–2345.
9 A. Tracz, J. K. Jeszka, M. D. Watson, W. Pisula, K. Müllen and T. Pakula, *J. Am. Chem. Soc.*, 2003, **125**, 1682–1683.
10 W. Pisula, A. Menon, M. Stepputat, I. Lieberwirth, U. Kolb, A. Tracz, H. Sirringhaus, T. Pakula and K. Müllen, *Adv. Mater.*, 2005, **17**, 684–689.
11 H. Monobe, K. Awazu and Y. Shimizu, *Adv. Mater.*, 2000, **12**, 1495–1499.
12 S. Zimmermann, J. H. Wendorff and C. Weder, *Chem. Mater.*, 2002, **14**, 2218–2223.
13 O. Bunk, M. M. Nielsen, T. I. Solling, A. M. van de Craats and N. Stutzmann, *J. Am. Chem. Soc.*, 2003, **125**, 2252–2258.
14 A. M. van de Craats, N. Stutzmann, O. Bunk, M. M. Nielsen, M. Watson, K. Müllen, H. D. Chanzy, H. Sirringhaus and R. H. Friend, *Adv. Mater.*, 2003, **15**, 495–499.
15 M. Funahashi and J.-i. Hanna, *Appl. Phys. Lett.*, 2000, **76**, 2574–2576.
16 M. O'Neill and S. M. Kelly, *Adv. Mater.*, 2003, **15**, 1135–1146.
17 J. Cornil, D. Beljonne, J.-P. Calbert and J.-L. Bredas, *Adv. Mater.*, 2001, **13**, 1053–1067.
18 J. Cornil, J. P. Calbert and J. L. Bredas, *J. Am. Chem. Soc.*, 2001, **123**, 1250–1251.
19 X. Crispin, J. Cornil, R. Friedlein, K. K. Okudaira, V. Lemaur, A. Crispin, G. Kestemont, M. Lehmann, M. Fahlman, R. Lazzaroni, Y. Geerts, G. Wendin, N. Ueno, J.-L. Bredas and W. R. Salaneck, *J. Am. Chem. Soc.*, 2004, **126**, 11889–11899.
20 J. M. Warman, M. P. de Haas, G. Dicker, F. C. Grozema, J. Piris and M. G. Debije, *Chem. Mater.*, 2004, **16**, 4600–4609.
21 Z. An, J. Yu, S. C. Jones, S. Barlow, S. Yoo, B. Domercq, P. Prins, L. D. A. Siebbeles, B. Kippelen and S. R. Marder, *Adv. Mater.*, 2005, **17**, 2580–2583.
22 B. A. Jones, M. J. Ahrens, M.-H. Yoon, A. Facchetti, T. J. Marks and M. R. Wasielewski, *Angew. Chem., Int. Ed.*, 2004, **43**, 6363–6366.
23 H. Iino, Y. Takayashiki, J.-i. Hanna and R. J. Bushby, *Jpn. J. Appl. Phys., Part 2*, 2005, **44**, L1310–L1312.
24 D. Markovitsi, S. Marguet, J. Bondkowski and S. Kumar, *J. Phys. Chem. B*, 2001, **105**, 1299–1306.
25 A. Hayer, V. de Halleux, A. Köhler, A. El-Garoughy, E. W. Meijer, J. Barbera, J. Tant, J. Levin, M. Lehmann, J. Gierschner, J. Cornil and Y. H. Geerts, *J. Phys. Chem. B*, 2006, **110**, 7653–7659.
26 V. de Halleux, J.-P. Calbert, P. Brocorens, J. Cornil, J.-P. Declercq, J.-L. Bredas and Y. Geerts, *Adv. Funct. Mater.*, 2004, **14**, 649–659.

27 N. B. McKeown, *Phthalocyanine Materials: Synthesis, Structure and Function*, University Press, Cambridge, 1998.
28 M. D. Watson, A. Fechtenkötter and K. Müllen, *Chem. Rev.*, 2001, **101**, 1267–1300.
29 A. N. Cammidge and R. J. Bushby, in *Handbook of Liquid Crystals*, ed. D. Demus, J. W. Goodby, G. W. Gray, H. W. Spiess and V. Vill, Wiley-WCH, Weinheim, 1998, vol. 2B, ch. 7, pp. 693–747.
30 S. Kumar, *Liq. Cryst.*, 2004, **31**, 1037–1059.
31 S. Kumar, *Chem. Soc. Rev.*, 2006, **35**, 83–109.
32 C.-y. Liu and A. J. Bard, *Acc. Chem. Res.*, 1999, **32**, 235–245.
33 N. Boden, R. J. Bushby, J. Clements and B. Movaghar, *J. Mater. Chem.*, 1999, **9**, 2081–2086.
34 T. Kato, N. Mizoshita and K. Kishimoto, *Angew. Chem., Int. Ed.*, 2006, **45**, 38–68.
35 H. Takezoe, K. Kishikawa and E. Gorecka, *J. Mater. Chem.*, 2006, **16**, 2412–2416.
36 R. J. Bushby and O. R. Lozman, *Curr. Opin. Colloid Interface Sci.*, 2002, **7**, 343–354.
37 S. Kumar, *Liq. Cryst.*, 2005, **32**, 1089–1113.
38 C. Piechocki, J. Simon, A. Skoulios, D. Guillon and P. Weber, *J. Am. Chem. Soc.*, 1982, **104**, 5245–5247.
39 D. Adam, P. Schuhmacher, J. Simmerer, L. Haussling, K. Siemensmeyer, K. H. Etzbach, H. Ringsdorf and D. Haarer, *Nature*, 1994, **371**, 141–143.
40 A. M. van de Craats, J. M. Warman, M. P. de Haas, D. Adam, J. Simmerer, D. Haarer and P. Schuhmacher, *Adv. Mater.*, 1996, **8**, 823–826.
41 A. M. van de Craats, M. P. de Haas and J. M. Warman, *Synth. Met.*, 1997, **86**, 2125–2126.
42 V. Lemaur, D. A. da Silva Filho, V. Coropceanu, M. Lehmann, Y. Geerts, J. Piris, M. G. Debije, A. M. van de Craats, K. Senthilkumar, L. D. A. Siebbeles, J. M. Warman, J.-L. Bredas and J. Cornil, *J. Am. Chem. Soc.*, 2004, **126**, 3271–3279.
43 J. F. van der Pol, E. Neeleman, J. W. Zwikker, R. J. M. Nolte, W. Drenth, J. Aerts, R. Visser and S. J. Picken, *Liq. Cryst.*, 1989, **6**, 577–592.
44 K. Ohta, L. Jacquemin, C. Sirlin, L. Bosio and J. Simon, *New J. Chem.*, 1988, **12**, 751–754.
45 D. Guillon, A. Skoulios, C. Piechocki, J. Simon and P. Weber, *Mol. Cryst. Liq. Cryst.*, 1983, **100**, 275–284.
46 L. Dulog and A. Gittinger, *Mol. Cryst. Liq. Cryst.*, 1992, **213**, 31–42.
47 S. Sergeyev, E. Pouzet, O. Debever, J. Levin, J. Gierschner, J. Cornil, R. Gomez-Aspe and Y. H. Geerts, *J. Mater. Chem.*, 2007, **17**, 1777–1784.
48 H. Eichhorn, *J. Porphyrins Phthalocyanines*, 2000, **4**, 88–102.
49 P. Herwig, C. W. Kayser, K. Müllen and H. W. Spiess, *Adv. Mater.*, 1996, **8**, 510–513.
50 V. S. Iyer, M. Wehmeier, J. D. Brand, M. A. Keegstra and K. Müllen, *Angew. Chem., Int. Ed. Engl.*, 1997, **36**, 1604–1607.
51 Z. Tomovic, M. D. Watson and K. Müllen, *Angew. Chem., Int. Ed.*, 2004, **43**, 755–758.
52 M. D. Watson, M. G. Debije, J. M. Warman and K. Müllen, *J. Am. Chem. Soc.*, 2004, **126**, 766–771.
53 V. S. Iyer, K. Yoshimura, V. Enkelmann, R. Epsch, J. P. Rabe and K. Müllen, *Angew. Chem., Int. Ed.*, 1998, **37**, 2696–2699.
54 M. G. Debije, J. Piris, M. P. de Haas, J. M. Warman, Z. Tomovic, C. D. Simpson, M. D. Watson and K. Müllen, *J. Am. Chem. Soc.*, 2004, **126**, 4641–4645.
55 A. M. van de Craats and J. M. Warman, *Adv. Mater.*, 2001, **13**, 130–133.
56 J. Cornil, V. Lemaur, J. P. Calbert and J. L. Bredas, *Adv. Mater.*, 2002, **14**, 726–729.
57 K. Senthilkumar, F. C. Grozema, F. M. Bickelhaupt and L. D. A. Siebbeles, *J. Chem. Phys.*, 2003, **119**, 9809–9817.
58 M. Lehmann, V. Lemaur, J. Cornil, J. L. Bredas, S. Goddard, I. Grizzi and Y. Geerts, *Tetrahedron*, 2004, **60**, 3283–3291.
59 S. P. Brown and H. W. Spiess, *Chem. Rev.*, 2001, **101**, 4125–4155.
60 I. Fischbach, T. Pakula, P. Minkin, A. Fechtenkötter, K. Müllen, H. W. Spiess and K. Saalwächter, *J. Phys. Chem. B*, 2002, **106**, 6408–6418.
61 O. Roussel, G. Kestemont, J. Tant, V. de Halleux, R. G. Aspe, J. Levin, A. Remacle, I. R. Gearba, D. Ivanov, M. Lehmann and Y. Geerts, *Mol. Cryst. Liq. Cryst.*, 2003, **396**, 35–39.
62 M. Lehmann, G. Kestemont, R. G. Aspe, C. Buess-Herman, M. H. J. Koch, M. G. Debije, J. Piris, M. P. de Haas, J. M. Warman, M. D. Watson, V. Lemaur, J. Cornil, Y. H. Geerts, R. Gearba and D. A. Ivanov, *Chem.–Eur. J.*, 2005, **11**, 3349–3362.
63 L. J. Lever, R. W. Kelsall and R. J. Bushby, *Phys. Rev. B*, 2005, **72**, 035130.
64 R. I. Gearba, M. Lehmann, J. Levin, D. A. Ivanov, M. H. J. Koch, J. Barbera, M. G. Debije, J. Piris and Y. H. Geerts, *Adv. Mater.*, 2003, **15**, 1614–1618.
65 V. Coropceanu, M. Malagoli, D. A. da Silva Filho, N. E. Gruhn, T. G. Bill and J. L. Bredas, *Phys. Rev. Lett.*, 2002, **89**, 275503.
66 W. A. Macdonald, *J. Mater. Chem.*, 2004, **14**, 4–10.
67 M. K. Engel, P. Bassoul, L. Bosio, H. Lehmann, M. Hanack and J. Simon, *Liq. Cryst.*, 1993, **15**, 709–722.
68 E. F. Gramsbergen, H. J. Hoving, W. H. Dejeu, K. Praefcke and B. Kohne, *Liq. Cryst.*, 1986, **1**, 397–400.
69 L. Y. Chiang, C. R. Safinya, N. A. Clark, K. S. Liang and A. N. Bloch, *J. Chem. Soc., Chem. Commun.*, 1985, 695–696.
70 P. G. Schouten, J. M. Warman, M. P. de Haas, C. F. van Nostrum, G. H. Gelinck, R. J. M. Nolte, M. J. Copyn, J. W. Zwikker, M. K. Engel, M. Hanack, Y. H. Chang and W. T. Ford, *J. Am. Chem. Soc.*, 1994, **116**, 6880–6894.
71 C. Y. Liu, A. Fechtenkötter, M. D. Watson, K. Müllen and A. J. Bard, *Chem. Mater.*, 2003, **15**, 124–130.
72 A. M. van de Craats, J. M. Warman, A. Fechtenkötter, J. D. Brand, M. A. Harbison and K. Müllen, *Adv. Mater.*, 1999, **11**, 1469–1472.
73 Y. Geerts, unpublished work.
74 J. Tant, Ph.D. Thesis, Université Libre de Bruxelles, 2004.
75 R. Gearba, A. I. Bondar, B. Goderis, W. Bras and D. A. Ivanov, *Chem. Mater.*, 2005, **17**, 2825–2832.
76 W. Pisula, M. Kastler, D. Wasserfallen, M. Mondeshki, J. Piris, I. Schnell and K. Müllen, *Chem. Mater.*, 2006, **18**, 3634–3640.
77 W. Pisula, M. Kastler, D. Wasserfallen, T. Pakula and K. Müllen, *J. Am. Chem. Soc.*, 2004, **126**, 8074–8075.
78 G. J. Clarkson, N. B. McKeown and K. E. Treacher, *J. Chem. Soc., Perkin Trans. 1*, 1995, 1817–1823.
79 D. M. Collard and C. P. Lillya, *J. Am. Chem. Soc.*, 1991, **113**, 8577–8583.
80 S. Kumar, D. S. S. Rao and S. K. Prasad, *J. Mater. Chem.*, 1999, **9**, 2751–2754.
81 A. Fechtenkötter, N. Tchebotareva, M. Watson and K. Müllen, *Tetrahedron*, 2001, **57**, 3769–3783.
82 N. Terasawa, N. Tanigaki, H. Monobe and K. Kiyohara, *J. Fluorine Chem.*, 2006, **127**, 1096–1104.
83 N. Terasawa, H. Monobe and K. Kiyohara, *J. Fluorine Chem.*, 2006, **127**, 954–961.
84 B. Alameddine, O. F. Aebischer, W. Amrein, B. Donnio, R. Deschenaux, D. Guillon, C. Savary, D. Scanu, O. Scheidegger and T. A. Jenny, *Chem. Mater.*, 2005, **17**, 4798–4807.
85 U. Dahn, C. Erdelen, H. Ringsdorf, R. Festag, J. H. Wendorff, P. A. Heiney and N. C. Maliszewskyj, *Liq. Cryst.*, 1995, **19**, 759–764.
86 N. Terasawa, H. Monobe, K. Kiyohara and Y. Shimizu, *Chem. Commun.*, 2003, 1678–1679.
87 A. Fechtenkötter, K. Saalwächter, M. A. Harbison, K. Müllen and H. W. Spiess, *Angew. Chem., Int. Ed.*, 1999, **38**, 3039–3042.
88 J. Wu, M. D. Watson and K. Müllen, *Angew. Chem., Int. Ed.*, 2003, **42**, 5329–5333.
89 J. Wu, M. D. Watson, L. Zhang, Z. H. Wang and K. Müllen, *J. Am. Chem. Soc.*, 2004, **126**, 177–186.
90 A. C. Grimsdale, J. Wu and K. Müllen, *Chem. Commun.*, 2005, 2197–2204.

91 J. Wu, M. Baumgarten, M. G. Debije, J. W. Warman and K. Müllen, *Angew. Chem., Int. Ed.*, 2004, **43**, 5331–5335.
92 J. Wu, J. Li, U. Kolb and K. Müllen, *Chem. Commun.*, 2006, 48–50.
93 M. Lee, J. W. Kim, S. Peleshanko, K. Larson, Y. S. Yoo, D. Vaknin, S. Markutsya and V. V. Tsukruk, *J. Am. Chem. Soc.*, 2002, **124**, 9121–9128.
94 E. M. Garcia-Frutos, G. Bottari, P. Vazquez, J. Barbera and T. Torres, *Chem. Commun.*, 2006, 3107–3109.
95 D. Perez and E. Guitian, *Chem. Soc. Rev.*, 2004, **33**, 274–283.
96 N. Boden, R. J. Bushby and A. N. Cammidge, *Liq. Cryst.*, 1995, **18**, 673–676.
97 S. Kumar and M. Manickam, *Chem. Commun.*, 1998, 1427–1428.
98 H. Bock, M. Rajaoarivelo, S. Clavaguera and E. Grelet, *Eur. J. Org. Chem.*, 2006, 2889–2893.
99 S. Ito, M. Wehmeier, J. D. Brand, C. Kübel, R. Epsch, J. P. Rabe and K. Müllen, *Chem.–Eur. J.*, 2000, **6**, 4327–4342.
100 W. Pisula, Z. Tomovic, C. Simpson, M. Kastler, T. Pakula and K. Müllen, *Chem. Mater.*, 2005, **17**, 4296–4303.
101 R. J. Bushby, I. W. Hamley, Q. Liu, O. R. Lozman and J. E. Lydon, *J. Mater. Chem.*, 2005, **15**, 4429–4434.
102 P. Samori, X. M. Yin, N. Tchebotareva, Z. H. Wang, T. Pakula, F. Jackel, M. D. Watson, A. Venturini, K. Müllen and J. P. Rabe, *J. Am. Chem. Soc.*, 2004, **126**, 3567–3575.
103 N. Tchebotareva, X. M. Yin, M. D. Watson, P. Samori, J. P. Rabe and K. Müllen, *J. Am. Chem. Soc.*, 2003, **125**, 9734–9739.
104 S. Kumar, J. J. Naidu and S. K. Varshney, *Mol. Cryst. Liq. Cryst.*, 2004, **411**, 1397–1404.
105 J. P. Hill, W. Jin, A. Kosaka, T. Fukushima, H. Ichihara, T. Shimomura, K. Ito, T. Hashizume, N. Ishii and T. Aida, *Science*, 2004, **304**, 1481–1483.
106 W. Jin, T. Fukushima, M. Niki, A. Kosaka, N. Ishii and T. Aida, *Proc. Natl. Acad. Sci. U. S. A.*, 2005, **102**, 10801–10806.
107 Y. Yamamoto, T. Fukushima, W. Jin, A. Kosaka, T. Hara, T. Nakamura, A. Saeki, S. Seki, S. Tagawa and T. Aida, *Adv. Mater.*, 2006, **18**, 1297–1300.
108 M. Kastler, J. Schmidt, W. Pisula, D. Sebastiani and K. Müllen, *J. Am. Chem. Soc.*, 2006, **128**, 9526–9534.
109 K. Lau, J. Foster and V. Williams, *Chem. Commun.*, 2003, 2172–2173.
110 E. J. Foster, R. B. Jones, C. Lavigueur and V. E. Williams, *J. Am. Chem. Soc.*, 2006, **128**, 8569–8574.
111 E. J. Foster, J. Babuin, N. Nguyen and V. E. Williams, *Chem. Commun.*, 2004, 2052–2053.
112 F. Würthner, *Chem. Commun.*, 2004, 1564–1579.
113 H. Langhals, *Helv. Chim. Acta*, 2005, **88**, 1309–1343.
114 C. W. Struijk, A. B. Sieval, J. E. J. Dakhorst, M. van Dijk, P. Kimkes, R. B. M. Koehorst, H. Donker, T. J. Schaafsma, S. J. Picken, A. M. van de Craats, J. M. Warman, H. Zuilhof and E. J. R. Sudholter, *J. Am. Chem. Soc.*, 2000, **122**, 11057–11066.
115 G. Zucchi, B. Donnio and Y. H. Geerts, *Chem. Mater.*, 2005, **17**, 4273–4277.
116 F. Würthner, C. Thalacker, S. Diele and C. Tschierske, *Chem.–Eur. J.*, 2001, **7**, 2245–2253.
117 F. Nolde, W. Pisula, S. Müller, C. Kohl and K. Müllen, *Chem. Mater.*, 2006, **18**, 3715–3725.
118 U. Rohr, C. Kohl, K. Müllen, A. van de Craats and J. Warman, *J. Mater. Chem.*, 2001, **11**, 1789–1799.
119 S. Saidi-Besbes, E. Grelet and H. Bock, *Angew. Chem., Int. Ed.*, 2006, **45**, 1783–1786.
120 S. Benning, H. S. Kitzerow, H. Bock and M. F. Achard, *Liq. Cryst.*, 2000, **27**, 901–906.
121 T. Hassheider, S. A. Benning, H.-S. Kitzerow, M.-F. Achard and H. Bock, *Angew. Chem., Int. Ed.*, 2001, **40**, 2060–2063.
122 T. Hassheider, S. A. Benning, M. W. Lauhof, H. S. Kitzerow, H. Bock, M. D. Watson and K. Müllen, *Mol. Cryst. Liq. Cryst.*, 2004, **413**, 2597–2608.
123 S. Ito, P. T. Herwig, T. Böhme, J. P. Rabe, W. Rettig and K. Müllen, *J. Am. Chem. Soc.*, 2000, **122**, 7698–7706.
124 L. Zhi, J. Wu and K. Müllen, *Org. Lett.*, 2005, **7**, 5761–5764.
125 M. D. Watson, F. Jäckel, N. Severin, J. P. Rabe and K. Müllen, *J. Am. Chem. Soc.*, 2004, **126**, 1402–1407.
126 K. Hatsusaka, N. Kimura and K. Ohta, *Bull. Chem. Soc. Jpn.*, 2003, **76**, 781–787.
127 K. Ohta, K. Hatsusaka, M. Sugibayashi, M. Ariyoshi, K. Ban, F. Maeda, R. Naito, K. Nishizawa, A. M. van de Craats and J. M. Warman, *Mol. Cryst. Liq. Cryst.*, 2003, **397**, 325–345.
128 D. Guillon, *Struct. Bonding*, 1999, **95**, 41–82.
129 V. Percec, M. Glodde, T. K. Bera, Y. Miura, I. Shiyanovskaya, K. D. Singer, V. S. K. Balagurusamy, P. A. Heiney, I. Schnell, A. Rapp, H. W. Spiess, S. D. Hudson and H. Duan, *Nature*, 2002, **419**, 384–387.
130 C. A. Hunter and J. K. M. Sanders, *J. Am. Chem. Soc.*, 1990, **112**, 5525–5534.
131 C. Tschierske, *J. Mater. Chem.*, 2001, **11**, 2647–2671.
132 W. Pisula, M. Kastler, Y. Changduk, V. Enkelmann and K. Müllen, *Chem.–Asian J.*, 2007, **2**, 51–56.
133 C. Ochsenfeld, S. P. Brown, I. Schnell, J. Gauss and H. W. Spiess, *J. Am. Chem. Soc.*, 2001, **123**, 2597–2606.
134 N. Boden, R. J. Bushby, G. Cooke, O. R. Lozman and Z. B. Lu, *J. Am. Chem. Soc.*, 2001, **123**, 7915–7916.
135 T. Kreouzis, K. Scott, K. J. Donovan, N. Boden, R. J. Bushby, O. R. Lozman and Q. Liu, *Chem. Phys.*, 2000, **262**, 489–497.
136 L. Y. Park, D. G. Hamilton, E. A. McGehee and K. A. McMenimen, *J. Am. Chem. Soc.*, 2003, **125**, 10586–10590.
137 W. Pisula, M. Kastler, D. Wasserfallen, J. W. F. Robertson, F. Nolde, C. Kohl and K. Müllen, *Angew. Chem., Int. Ed.*, 2006, **45**, 819–823.
138 M. L. Bushey, T.-Q. Nguyen, W. Zhang, D. Horoszewski and C. Nuckolls, *Angew. Chem., Int. Ed.*, 2004, **43**, 5446–5453.
139 D. Wasserfallen, I. Fischbach, N. Chebotareva, M. Kastler, W. Pisula, F. Jäckel, M. D. Watson, I. Schnell, J. P. Rabe, H. W. Spiess and K. Müllen, *Adv. Funct. Mater.*, 2005, **15**, 1585–1594.
140 P. H. J. Kouwer, W. F. Jager, W. J. Mijs and S. J. Picken, *J. Mater. Chem.*, 2003, **13**, 458–469.
141 K. Singh, S. Singh and T. K. Lahiri, *Liq. Cryst.*, 2000, **27**, 1431–1436.
142 P. H. J. Kouwer, O. van den Berg, W. F. Jager, W. J. Mijs and S. J. Picken, *Macromolecules*, 2002, **35**, 2576–2582.
143 Y. Shimizu, A. Kurobe, H. Monobe, N. Terasawa, K. Kiyohara and K. Uchida, *Chem. Commun.*, 2003, 1676–1677.
144 K. Kawata, *Chem. Rec.*, 2002, **2**, 59–80.
145 A. M. Levelut, *J. Chem. Phys.*, 1983, **88**, 149–161.
146 B. Glusen, W. Heitz, A. Kettner and J. H. Wendorff, *Liq. Cryst.*, 1996, **20**, 627–633.
147 J. Simmerer, B. Glusen, W. Paulus, A. Kettner, P. Schuhmacher, D. Adam, K. H. Etzbach, K. Siemensmeyer, J. H. Wendorff, H. Ringsdorf and D. Haarer, *Adv. Mater.*, 1996, **8**, 815–819.
148 N. Boden, R. J. Bushby, J. Clements, K. Donovan, B. Movaghar and T. Kreouzis, *Phys. Rev. B*, 1998, **58**, 3063–3074.
149 M. Lehmann, I. Fischbach, H. W. Spiess and H. Meier, *J. Am. Chem. Soc.*, 2004, **126**, 772–784.
150 I. Fischbach, F. Ebert, H. W. Spiess and I. Schnell, *ChemPhysChem*, 2004, **5**, 895–908.
151 B. Schartel, A. Kettner, R. Kunze, J. H. Wendorff and M. Hennecke, *Adv. Mater. Opt. Electron.*, 1999, **9**, 55–64.
152 H. Sirringhaus, P. J. Brown, R. H. Friend, M. M. Nielsen, K. Bechgaard, B. M. W. Langeveld-Voss, A. J. H. Spiering, R. A. J. Janssen, E. W. Meijer, P. Herwig and D. M. de Leeuw, *Nature*, 1999, **401**, 685–688.
153 N. R. Armstrong, *J. Porphyrins Phthalocyanines*, 2000, **4**, 414–417.
154 S. D. Xu, Q. D. Zeng, J. Lu, C. Wang, L. J. Wan and C. L. Bai, *Surf. Sci.*, 2003, **538**, L451–L459.
155 F. Charra and J. Cousty, *Phys. Rev. Lett.*, 1998, **80**, 1682–1685.
156 M. Palma, J. Levin, V. Lemaur, A. Liscio, V. Palermo, J. Cornil, Y. Geerts, M. Lehmann and P. Samorì, *Adv. Mater.*, 2006, **18**, 3313–3317.
157 R. Friedlein, X. Crispin, C. D. Simpson, M. D. Watson, F. Jäckel, W. Osikowicz, S. Marciniak, M. P. de Jong, P. Samori, S. K. M. Jonsson, M. Fahlman, K. Müllen, J. P. Rabe and W. R. Salaneck, *Phys. Rev. B*, 2003, **68**, 195414.
158 N. Boden, R. J. Bushby, P. S. Martin, S. D. Evans, R. W. Owens and D. A. Smith, *Langmuir*, 1999, **15**, 3790–3797.

159 A. Huijser, T. J. Savenije, A. Kotlewski, S. J. Picken and L. D. A. Siebbeles, *Adv. Mater.*, 2006, **18**, 2234–2239.
160 K. Hatsusaka, K. Ohta, I. Yamamoto and H. Shirai, *J. Mater. Chem.*, 2001, **11**, 423–433.
161 W. Pisula, Ž. Tomovic, B. El Hamaoui, M. D. Watson, T. Pakula and K. Müllen, *Adv. Funct. Mater.*, 2005, **15**, 893–904.
162 E. Grelet and H. Bock, *Europhys. Lett.*, 2006, **73**, 712–718.
163 V. de Cupere, C. Heintz, Y. Geerts and J. Tant, *Eur. Pat.*, 1722424, 2006.
164 R. J. Bushby, S. D. Evans, O. R. Lozman, A. McNeill and B. Movaghar, *J. Mater. Chem.*, 2001, **11**, 1982–1984.
165 J. M. Kroon, R. B. M. Koehorst, M. van Dijk, G. M. Sanders and E. J. R. Sudholter, *J. Mater. Chem.*, 1997, **7**, 615–624.
166 A. N. Cammidge and H. Gopee, *J. Mater. Chem.*, 2001, **11**, 2773–2783.
167 H. Bock, A. Babeau, I. Seguy, P. Jolinat and P. Destruel, *ChemPhysChem*, 2002, **6**, 532–535.
168 H. Eichhorn, D. W. Bruce and D. Wöhrle, *Adv. Mater.*, 1998, **10**, 419–422.
169 D. Wasserfallen, M. Kastler, W. Pisula, W. A. Hofer, Y. Fogel, Z. Wang and K. Müllen, *J. Am. Chem. Soc.*, 2006, **128**, 1334–1339.
170 M. Yoshio, T. Kagata, K. Hoshino, T. Mukai, H. Ohno and T. Kato, *J. Am. Chem. Soc.*, 2006, **128**, 5570–5577.
171 J. Hoogboom, P. M. L. Garcia, M. B. J. Otten, J. A. A. W. Elemans, J. Sly, S. V. Lazarenko, T. Rasing, A. E. Rowan and R. J. M. Nolte, *J. Am. Chem. Soc.*, 2005, **127**, 11047–11052.
172 K. Q. Jian, H. S. Shim, D. Tuhus-Dubrow, S. Bernstein, C. Woodward, M. Pfeffer, D. Steingart, T. Gournay, S. Sachsmann, G. P. Crawford and R. H. Hurt, *Carbon*, 2003, **41**, 2073–2083.
173 H. Monobe, K. Awazu and Y. Shimizu, *Adv. Mater.*, 2006, **18**, 607–610.
174 J. K. Vij, A. Kocot and T. S. Perova, *Mol. Cryst. Liq. Cryst.*, 2003, **397**, 531–544.
175 G. Kruk, A. Kocot, R. Wrzalik, J. K. Vij, O. Karthaus and H. Ringsdorf, *Liq. Cryst.*, 1993, **14**, 807–819.
176 C. Deibel, D. Janssen, P. Heremans, V. de Cupere, Y. Geerts, M. L. Benkhedir and G. J. Adriaenssens, *Org. Electron.*, 2006, **7**, 495–499.
177 M. Kastler, W. Pisula, F. Laquai, A. Kumar, R. J. Davies, S. Baluschev, M.-C. Garcia-Gutierrez, D. Wasserfallen, H.-J. Butt, C. Riekel, G. Wegner and K. Müllen, *Adv. Mater.*, 2006, **18**, 2255–2259.
178 T. Bjornholm, T. Hassenkam and N. Reitzel, *J. Mater. Chem.*, 1999, **9**, 1975–1990.
179 N. C. Maliszewskyj, P. A. Heiney, J. Y. Josefowicz, J. P. McCauley and A. B. Smith, *Science*, 1994, **264**, 77–79.
180 N. Reitzel, T. Hassenkam, K. Balashev, T. R. Jensen, P. B. Howes, K. Kjaer, A. Fechtenkötter, N. Tchebotareva, S. Ito, K. Müllen and T. Bjornholm, *Chem.–Eur. J.*, 2001, **7**, 4894–4901.
181 P. Henderson, D. Beyer, U. Jonas, O. Karthaus, H. Ringsdorf, P. A. Heiney, N. C. Maliszewskyj, S. S. Ghosh, O. Y. Mindyuk and J. Y. Josefowicz, *J. Am. Chem. Soc.*, 1997, **119**, 4740–4748.
182 S. Kubowicz, A. F. Thünemann, T. M. Geue, U. Pietsch, M. D. Watson, N. Tchebotareva and K. Müllen, *Langmuir*, 2003, **19**, 10997–10999.
183 A. F. Thünemann, S. Kubowicz, C. Burger, M. D. Watson, N. Tchebotareva and K. Müllen, *J. Am. Chem. Soc.*, 2003, **125**, 352–356.
184 P. Smolenyak, R. Peterson, K. Nebesny, M. Torker, D. F. O'Brien and N. R. Armstrong, *J. Am. Chem. Soc.*, 1999, **121**, 8628–8636.
185 R. A. P. Zangmeister, D. F. O'Brien and N. R. Armstrong, *Adv. Funct. Mater.*, 2002, **12**, 179–186.
186 S. Fouriaux, F. Armand, O. Araspin, A. RuaudelTeixier, E. M. Maya, P. Vazquez and T. Torres, *J. Phys. Chem.*, 1996, **100**, 16984–16988.
187 H. Nakahara, K. Z. Sun and K. Fukuda, *J. Mater. Chem.*, 1995, **5**, 395–399.
188 M. Duati, C. Grave, N. Tcbeborateva, J. Wu, K. Müllen, A. Shaporenko, M. Zharnikov, J. K. Kriebel, G. M. Whitesides and M. A. Rampi, *Adv. Mater.*, 2006, **18**, 329–333.
189 J. C. Wittmann and C. Smith, *Nature*, 1991, **352**, 414–417.
190 J. Piris, M. G. Debije, N. Stutzmann, A. M. van de Craats, M. K. Müllen and J. M. Warman, *Adv. Mater.*, 2003, **15**, 1736–1740.
191 A. Tracz, T. Pakula and J. K. Jeszka, *Mater. Sci.*, 2004, **22**, 415–421.
192 M. Kastler, W. Pisula, D. Wasserfallen, T. Pakula and K. Müllen, *J. Am. Chem. Soc.*, 2005, **127**, 4286–4296.
193 W. Pisula, Z. Tomovic, M. Stepputat, U. Kolb, T. Pakula and K. Müllen, *Chem. Mater.*, 2005, **17**, 2641–2647.
194 D. W. Breiby, F. Hansteen, W. Pisula, O. Bunk, U. Kolb, J. W. Andreasen, K. Müllen and M. M. Nielsen, *J. Phys. Chem. B*, 2005, **109**, 22319–22325.
195 D. W. Breiby, O. Bunk, W. Pisula, T. I. Solling, A. Tracz, T. Pakula, K. Müllen and M. M. Nielsen, *J. Am. Chem. Soc.*, 2005, **127**, 11288–11293.
196 J. Piris, M. G. Debije, N. Stutzmann, B. W. Laursen, W. Pisula, M. D. Watson, T. Bjornholm, K. Müllen and J. M. Warman, *Adv. Funct. Mater.*, 2004, **14**, 1053–1061.
197 C. Y. Liu and A. J. Bard, *Chem. Mater.*, 2000, **12**, 2353–2362.
198 M. Steinhart, S. Zimmermann, P. Göring, A. K. Schaper, U. Gösele, C. Weder and J. H. Wendorff, *Nano Lett.*, 2005, **5**, 429–434.
199 M. Steinhart, S. Murano, A. K. Schaper, T. Ogawa, M. Tsuji, U. Gösele, C. Weder and J. H. Wendorff, *Adv. Funct. Mater.*, 2005, **15**, 1656–1664.
200 W. Pisula, M. Kastler, D. Wasserfallen, R. J. Davies, M.-C. Garcia-Gutierrez and K. Müllen, *J. Am. Chem. Soc.*, 2006, **128**, 14424–14425.
201 L. Zhi, J. Wu, J. Li, U. Kolb and K. Müllen, *Angew. Chem., Int. Ed.*, 2005, **44**, 2120–2123.
202 V. Duzhko, H. Shi, K. D. Singer, A. N. Semyonov and R. J. Twieg, *Langmuir*, 2006, **22**, 7947–7951.
203 V. Duzhko and K. D. Singer, *J. Phys. Chem. C*, 2007, **111**, 27–31.
204 J. M. Warman and A. M. van de Craats, *Mol. Cryst. Liq. Cryst.*, 2003, **396**, 41–72.
205 A. M. van de Craats, J. M. Warman, K. Müllen, Y. Geerts and J. D. Brand, *Adv. Mater.*, 1998, **10**, 36–38.
206 N. Boden, R. J. Bushby and J. Clements, *J. Chem. Phys.*, 1993, **98**, 5920–5931.
207 N. Boden, R. J. Bushby, A. N. Cammidge, J. Clements, R. Luo and K. J. Donovan, *Mol. Cryst. Liq. Cryst.*, 1995, **261**, 251–257.
208 D. Adam, F. Closs, T. Frey, D. Funhoff, D. Haarer, H. Ringsdorf, P. Schuhmacher and K. Siemensmeyer, *Phys. Rev. Lett.*, 1993, **70**, 457–460.
209 R. J. Bushby and O. R. Lozman, *Curr. Opin. Solid State Mater. Sci.*, 2002, **6**, 569–578.
210 J. M. Warman, J. Piris, W. Pisula, M. Kastler, D. Wasserfallen and K. Müllen, *J. Am. Chem. Soc.*, 2005, **127**, 14257–14262.
211 I. Paraschiv, M. Giesbers, B. Van Lagen, F. C. Grozema, R. D. Abellon, L. D. A. Siebbeles, A. T. M. Marcelis, H. Zuilhof and E. J. R. Sudhoelter, *Chem. Mater.*, 2006, **18**, 968–974.
212 H. Iino, J. Hanna, R. J. Bushby, B. Movaghar, B. J. Whitaker and M. J. Cook, *Appl. Phys. Lett.*, 2005, **87**, 132102.
213 H. Iino, J. Hanna, C. Jäger and D. Haarer, *Mol. Cryst. Liq. Cryst.*, 2005, **436**, 1171–1178.
214 H. Iino, J. Hanna and D. Haarer, *Phys. Rev. B*, 2005, **72**, 193203.
215 H. Iino, Y. Takayashiki, J. Hanna, R. J. Bushby and D. Haarer, *Appl. Phys. Lett.*, 2005, **87**, 192105.
216 D. M. de Leeuw, M. M. J. Simenon, A. R. Brown and R. E. F. Einerhand, *Synth. Met.*, 1997, **87**, 53–59.
217 A. Rybak, J. Pfleger, J. Jung, M. Pavlik, I. Glowacki, J. Ulanski, Z. Tomovic, K. Müllen and Y. Geerts, *Synth. Met.*, 2006, **156**, 302–309.
218 M. A. Palenberg, R. J. Silbey, M. Malagoli and J. L. Bredas, *J. Chem. Phys.*, 2000, **112**, 1541–1546.
219 A. Ochse, A. Kettner, J. Kopitzke, J. H. Wendorff and H. Bassler, *Phys. Chem. Chem. Phys.*, 1999, **1**, 1757–1760.
220 V. Duzhko, A. Semyonov, R. J. Twieg and K. D. Singer, *Phys. Rev. B*, 2006, **73**, 064201.
221 C.-y. Liu and A. J. Bard, *Nature*, 2002, **418**, 162–164.

222 C. L. Donley, R. A. P. Zangmeister, X. Wei, B. Minch, A. Drager, S. K. Cherian, L. LaRussa, B. Kippelen, B. Domercq, D. L. Mathine, D. F. O'Brien and N. R. Armstrong, *J. Mater. Res.*, 2004, **19**, 2087–2099.
223 S. Cherian, C. Donley, D. Mathine, L. LaRussa, W. Xia and N. Armstrong, *J. Appl. Phys.*, 2004, **96**, 5638–5643.
224 B. A. Gregg, *J. Phys. Chem. B*, 2003, **107**, 4688–4698.
225 J. J. M. Halls, C. A. Walsh, N. C. Greenham, E. A. Marseglia, R. H. Friend, S. C. Moratti and A. B. Holmes, *Nature*, 1995, **376**, 498–500.
226 K. Petritsch, R. H. Friend, A. Lux, G. Rozenberg, S. C. Moratti and A. B. Holmes, *Synth. Met.*, 1999, **102**, 1776–1777.
227 M. Oukachmih, P. Destruel, I. Seguy, G. Ablart, P. Jolinat, S. Archambeau, M. Mabiala, S. Fouet and H. Bock, *Sol. Energy Mater.*, 2005, **85**, 535–543.
228 L. Schmidt-Mende, A. Fechtenkotter, K. Müllen, E. Moons, R. H. Friend and J. D. MacKenzie, *Science*, 2001, **293**, 1119–1122.
229 L. Schmidt-Mende, A. Fechtenkotter, K. Müllen, R. H. Friend and J. D. MacKenzie, *Phys. E: (Amsterdam, Neth.)*, 2002, **14**, 263–267.
230 J. P. Schmidtke, R. H. Friend, M. Kastler and K. Müllen, *J. Chem. Phys.*, 2006, **124**, 174704.
231 I. Seguy, P. Jolinat, P. Destruel, J. Farenc, R. Mamy, H. J. Bock and T. P. Nguyen, *J. Appl. Phys.*, 2001, **89**, 5442–5448.
232 G. Lussem and J. H. Wendorff, *Polym. Adv. Technol.*, 1998, **9**, 443–460.
233 I. Seguy, P. Destruel and H. Bock, *Synth. Met.*, 2000, **111–112**, 15–18.
234 I. H. Stapff, V. Stumpflen, J. H. Wendorff, D. B. Spohn and D. Mobius, *Liq. Cryst.*, 1997, **23**, 613–617.